Chapter 13
Shock Response Fixture Developed from Analytical and Experimental Data and Customized Using Structural Dynamics Modification Techniques

Kai Aizawa and Peter Avitabile

Abstract In order to characterize the acceleration response of a structure due to shock environments, the Shock Response Spectrum method is widely used in the qualification process for the spacecraft industry. Generally, this test is performed with a shock testing machine but alternate test fixture designs, including a shock plate, have recently been considered. In order to develop an appropriate design methodology to design such a fixture, a simple beam type structure is utilized to deploy the approach; the beam is chosen so as to introduce the SRS method into an educationally motivated treatment of the material for use in a graduate level course.

In this paper, the development of a Shock Response Spectrum for a beam-type structure from both analytical and experimental approaches is presented. From these models, frequencies, damping and mode shapes can be extracted to identify the response at various locations on the structure that are needed to develop the Shock Response Spectrum. In order to customize the shock spectrum, various mass perturbations applied to the structure can be considered by using Mass Sensitivity Analysis. The effects of the changes to the mass of the basic shock test fixture can be easily developed by using the Structural Dynamic Modification technique.

A comparison of the Shock Response Spectrum computed from the Analytical Model and from the Experimental Model is provided for various scenarios of different configurations studied.

Keywords Shock response spectrum (SRS) • Experimental and analytical SRS

Nomenclature

[M]	Mass matrix in physical space
[K]	Stiffness matrix in physical space
[C]	Damping matrix in physical space
$[\overline{M}]$	Mass matrix in modal space
$[\overline{K}]$	Stiffness matrix in modal space
$[\overline{C}]$	Damping matrix in modal space
[U]	Mode shapes
[λ]	Eigenvalues
X	Physical displacement in time domain
$\ddot{X}$	Physical Acceleration in time domain
F	Time vector of applied force
P	Modal displacement in time domain
$\ddot{p}$	Modal acceleration in time domain
$X(s)\|_{s=j\omega}$	Physical displacement in frequency domain

K. Aizawa
Acoustic Systems Laboratory (CAMAL), Chuo University, 1-13-27 Kasuga, Bunkyo-ku, Tokyo 112-8551, Japan

P. Avitabile (✉)
Structural Dynamics and Acoustic Systems Laboratory, University of Massachusetts Lowell, One University Avenue, Lowell, MA 01854, USA
e-mail: peteravitabile@uml.edu

G. Foss and C. Niezrecki (eds.), *Special Topics in Structural Dynamics, Volume 6: Proceedings of the 32nd IMAC, A Conference and Exposition on Structural Dynamics, 2014*, Conference Proceedings of the Society for Experimental Mechanics Series,
DOI 10.1007/978-3-319-04729-4_13,

$\ddot{X}(s)\big|_{s=j\omega}$ Physical acceleration in frequency domain
$H(s)|_{s=j\omega}$ Frequency response Function (FRF)
$[\Delta M]$ Mass modification matrix in physical space
$[\Delta K]$ Stiffness modification matrix in physical space

13.1 Introduction

13.1.1 Background

The Shock Response Spectrum has been widely used in the aerospace industry for many years to address many shock conditions including pyroshock which is a very high amplitude and short duration pulse. For more than 50 years, NASA has used the SRS for the majority of qualification of equipment used in a shock environment. While analyses can be performed, at some point the structure must be subjected to these shock loads in a laboratory environment. A variety of different shock machines have been developed to support this qualification effort.

NASA has created a standard to estimate the maximum shock value [1]. This standard facilitates the shock test and allows engineers to develop an input pulse that will cause the desired or specified shock spectrum. By using this standard, engineers can identify a possible maximum response on the structure with an arbitrary natural frequency and determine whether the structure can withstand the shock or not. The spectrum obtained by this standard is called the Shock Response Spectrum (SRS) and is used to determine suitability of equipment for different applications. The SRS was first developed in the U.S. Department of Defense and now defined in ISO 18431-4 [2] and an example of SRS is shown in Fig. 13.1. A SRS consists of a series of maximum acceleration response which is caused by an input force applied to a discrete number of single degree of freedom (SDOF) systems.

Typically the SRS is developed with a vibration shaker or a specifically designed shock machine. These machines are very specific and typically the cost to conduct these tests is very high. Recently [5], alternate methods have been considered to conduct this shock test that is less expensive to run. Specifically a SRS plate has been considered [5] and some preliminary studies have shown that this is a viable and economical approach to conducting SRS tests. That work showed some of the basic approaches to use the finite element (FE) model to identify the basic shock performance of the shock plate. But in order to customize the SRS, attachment masses need to be moved around the structure to obtain the desired SRS; extensive work was not performed in that earlier work nor was any optimal configuration studied or identified. But the customization of the specific spectrum does require some effort.

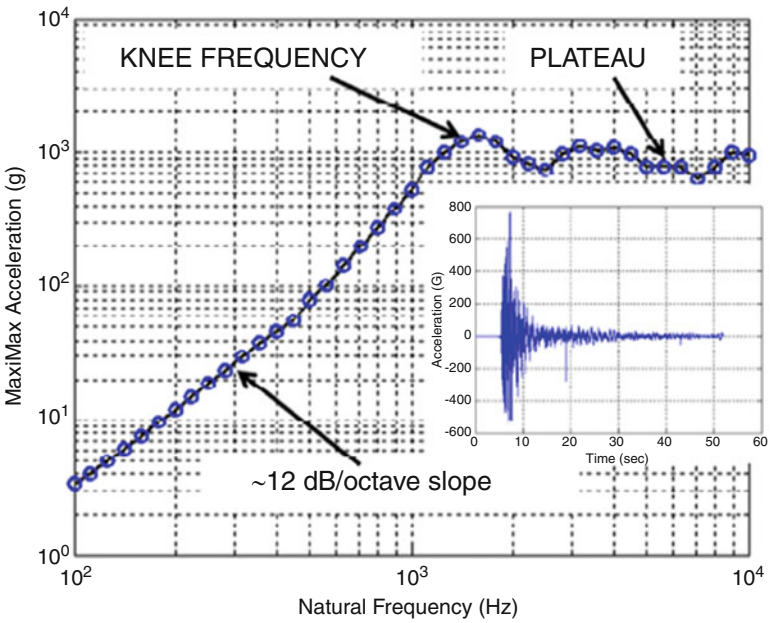

Fig. 13.1 Input pulse and calculated SRS for pyroshock (from [1])

In order to develop a methodology which can be useful for customizing SRS characteristics, in this paper, a simple beam will be used for the development of both experiment and analytical models. The beam is selected mainly as a "proof of concept" for the methodology presented and is not intended to be the final shock test configuration; ultimately the plate configuration studied in [5] is the more practical configuration. The main reason for selecting the beam is to use this shock test machine design as an educational tool for the study of vibration, shock and related topics necessary to perform these shock type calculations. In addition to the beam model, a more basic 5-degree of freedoms (DOF) analytical model will be used to determine proper configurations and to test some methodologies in this work and to illustrate some key points.

The design of the shock test machine involves the identification of the frequencies and mode shapes of the structure. This basic information is used for the prediction of the response of the set of SDOF systems that describe the structure and their response due to the shock excitation. The peak response of each of these SDOF systems are used to define the envelope of the SRS curve; mode contribution effects help to clearly see how individual modes affect the overall SRS curve desired. However, the SRS for the structure may not achieve the desired SRS and modifications may need to be considered. One very effective way to accomplish this is to use the Device Under Test (DUT) mounting block as a variable and movable mass which can be modified and attached at different locations to achieve different overall SRS at different points on the structure and/or introduce additional masses to attach to the structure.

To perform this mass modification, the Structural Dynamics Modification (SDM) will be conducted along with the Mass Sensitivity Analysis (MSA). In order to verify the relationship between each mode and each peak of the SRS, contribution analysis will also be used in this procedure. These will be performed for the FE model as well as an experimental configuration to show the benefits of using both analytical and experimental approaches to address the development of the SRS. The FE model is very useful in the design stage of the shock test fixture whereas the experimental approach helps to accurately predict the actual performance characteristics of the actual hardware configuration.

13.1.2 Motivation

In the previous paper [5], some numerical configurations for a proper FE model development were discussed. In that work, the effects of different damping values and the effects of the number of modes used for the SRS computation were studied. This was very useful but the earlier work did not adequately consider the experimental data as part of the development of the SRS; this was mainly due to the lack of correlation to the measured data and was not further studied or used for the SRS computation. However, there were some useful experimental mass modifications explored that clearly show the significant effect on the envelope of the SRS but only a few different configurations were explored in a somewhat random manner and optimization of the SRS spectrum was not considered in that work. Clearly more work can be performed to better understand the SRS spectrum and how it is developed from contribution of the different modes of the shock fixture and how to modify the structure to achieve certain performance goals. Due to this, a basic methodology to simulate a configuration of the SRS fixture will be discussed in this paper. Furthermore, a useful methodology to customize the SRS using optimized mass modification will be presented. Understanding these methodologies will be able to help design a proper SRS fixture and modify the SRS so that an acceptable configuration to satisfy the SRS envelop will be achieved.

13.2 Methodology

There are two main goals for this project: developing an appropriate methodology which is useful to simulate a shock response fixture and SRS customization to get the desired SRS. To perform this work, tools such as modal analysis, structure dynamics modification, time response computation and SRS computation are needed; the complete flow of analysis is summarized in Fig. 13.2. Modal parameters will be obtained from the Finite Element Analysis (FEA) or Experimental Modal Analysis (EMA). These parameters will be compared to each other and experimental modal damping values will be used in the FE model to simulate a proper experimental configuration. Using these verified modal parameters, the SDM, including the MSA to identify optimal location for mass modification, will be performed in case of the customization procedure. With these original or modified modal parameters, a direct time integration method using modal solution or an Inverse Fourier Transform (IFT) method will be performed to obtain the physical response. In addition, an acceleration signal is also measured with an actual experiment to compare the analytical model and measured structure data. These original or modified response signals from the FEA, EMA and an experiment will be treated as an input acceleration signal to compute the SRS. Then, a set of SRS envelopes obtained will be compared and the methodology proposed in this paper for the SRS computation and the SRS modification will be verified along with these results.

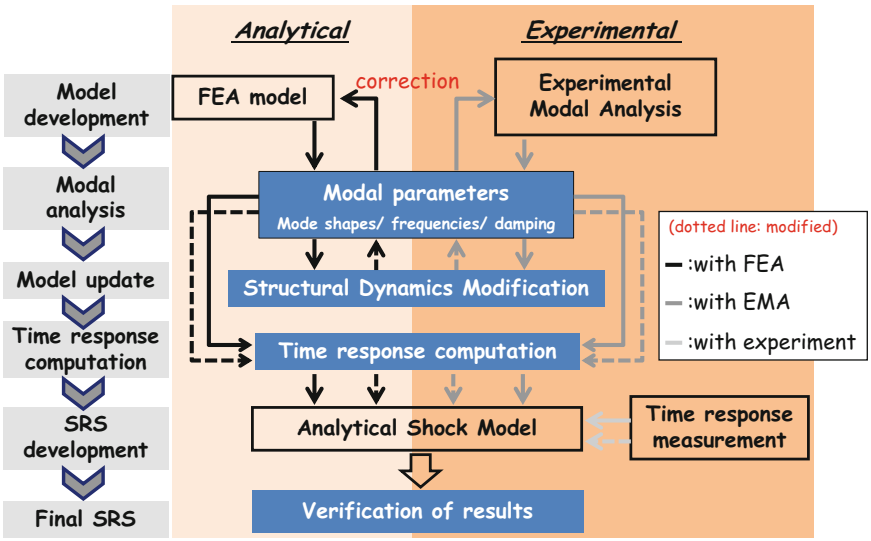

Fig. 13.2 Flow chart for this research

13.3 Theoretical Background

The background theories related to all the analyses are briefly described in this section. Because a time response will be required to develop a SRS, two methods will be examined to obtain the time response: the time domain and the frequency domain solution. The various related analyses to accomplish this work are described in separate sections identified as:

1. Equation of Motion and Modal Space Representation
2. Time Response Computation with Modal Superposition Technique in Time Domain
3. Time Response Computation with Frequency Response Function (FRF) in Frequency Domain
4. Shock Response Spectrum (SRS)
5. Contribution Analysis and Mass Sensitivity Analysis (MSA)
6. Structure Dynamics Modification (SDM)

The background theory and description of each of these follow.

13.3.1 Equation of Motion and Modal Space Representation

The equation of motion in physical space is used for the development of the FE model but the solutions are cast in modal space for easy computation as well as identifying a clear effect of the contribution that each mode makes to the overall response. The benefit of using the modal space solution is that the computation may be performed faster than the physical solution because the number of modes used for the computation is much smaller than the total number of DOFs (nDOF) in the FE model. The equation of motion in physical space for a multiple degree of freedoms (MDOF) system can be written as

$$[M]\{\ddot{X}\} + [C]\{\dot{X}\} + [K]\{X\} = \{F\} \tag{13.1}$$

The eigensolution of this system is written as

$$[[K] - \lambda_i [M]]\{X\} = \{0\} \tag{13.2}$$

From Eq. 13.2, eigenvalues λ and eigenvectors U will be obtained. Using these eigenvectors, the physical MDOF system set of equations can be uncoupled. The transformation from physical coordinates into modal coordinates is written as

$$\{X\} = [U]\{p\} \tag{13.3}$$

Substituting Eq. 13.3 into Eq. 13.1 and pre-multiplying $[U]^T$ in Eq. 13.1 results in

$$\left[\overline{M}\right]\{\ddot{p}\} + \left[\overline{C}\right]\{\dot{p}\} + \left[\overline{K}\right]\{p\} = [U]^T\{F\} \tag{13.4}$$

This represents the equation of motion in modal space and will be used for direct time integration to compute the physical acceleration. If the mode shape is scaled to the unit modal mass, due to the orthogonality and linear independence, the transformation from physical space to modal space will provide the modal mass and stiffness matrices written as follows

$$\left[U^T\right][M][U] = \begin{bmatrix} \ddots & & \\ & \overline{M} & \\ & & \ddots \end{bmatrix} \rightarrow \begin{bmatrix} \ddots & & \\ & I & \\ & & \ddots \end{bmatrix} \tag{13.5}$$

$$\left[U^T\right][K][U] = \begin{bmatrix} \ddots & & \\ & \overline{K} & \\ & & \ddots \end{bmatrix} \rightarrow \begin{bmatrix} \ddots & & \\ & \omega^2 & \\ & & \ddots \end{bmatrix} \tag{13.6}$$

The modal damping matrix can also be identified providing that proportional damping is assumed and written as

$$\left[U^T\right][C][U] = \begin{bmatrix} \ddots & & \\ & \overline{C} & \\ & & \ddots \end{bmatrix} \rightarrow \begin{bmatrix} \ddots & & \\ & 2\zeta\sqrt{\overline{M}\,\overline{K}} & \\ & & \ddots \end{bmatrix} \tag{13.7}$$

Here, ζ should not be a constant factor but be measured in an experiment to develop a proper SRS [5]. Due to this reason, a series of ζ for every one of the modes of interest will be selected from the EMA.

13.3.2 Time Response Computation with Modal Superposition Technique in Time Domain

The Newmark Direct Integration Method [7] is used to obtain a time response signal. This method uses a direct integration of the equation of motion in modal space shown in Eq. 13.1 with subscript of "$t = i$" as

$$\left[\overline{M}\right]\{\ddot{p}_{t=i}\} + \left[\overline{C}\right]\{\dot{p}_{t=i}\} + \left[\overline{K}\right]\{p_{t=i}\} = \left\{\overline{F}_{t=0}\right\}, \text{where } \left\{\overline{F}\right\} = [U]^T\{F\} \tag{13.8}$$

In order to achieve an acceleration response, the Newmark method will require the initial acceleration $\ddot{p}_{t=0}$ for the first step of computation and its form is written as

$$\{\ddot{p}_{t=0}\} = \left[\overline{M}\right]^{-1}\left[\left\{\overline{F}_{t=0}\right\} - \left[\overline{C}\right]\{\dot{p}_{t=0}\} - \left[\overline{K}\right]\{p_{t=0}\}\right] \tag{13.9}$$

Using these initial values for the displacement, velocity and acceleration, the displacement for the next time step is written using the constant factor α and β and time increment Δt as

$$\{p_{t=i+1}\} = \left[\frac{1}{\alpha(\Delta t)^2}[\overline{m}] + \frac{\beta}{\alpha\Delta t}[\overline{c}] + \left[\overline{k}\right]\right]^{-1} \begin{bmatrix} \left\{\overline{f}_{t=i+1}\right\} + [\overline{m}]\left(\frac{1}{\alpha(\Delta t)^2}\{p_{t=i}\} + \frac{1}{\alpha\Delta t}\{\dot{p}_{t=i}\} + \left(\frac{1}{2\alpha} - 1\right)\{\ddot{p}_{t=i}\}\right) \\ + \left[\overline{C}\right]\left(\frac{\beta}{\alpha\Delta t}\{p_{t=i}\} + \left(\frac{\beta}{\alpha} - 1\right)\{\dot{p}_{t=i}\} + \left(\frac{\beta}{\alpha} - 2\right)\frac{\Delta t}{2}\{\ddot{p}_{t=i}\}\right) \end{bmatrix},$$

$$where\ i = 0, 1, 2 \ldots, maximum\ time\ length \tag{13.10}$$

Then, the acceleration for the same time step is calculated using the displacement obtained for the next time step and the initial conditions for the displacement, velocity and acceleration using

$$\ddot{p}_{t=i+1} = \frac{1}{\alpha(\Delta t)^2}\left(\{p_{t=i+1}\} - \{p_{t=i}\}\right) - \frac{1}{\alpha\Delta t}\{\dot{p}_{t=i}\} - \left(\frac{1}{2\alpha} - 1\right)\{\ddot{p}_{t=i}\} \tag{13.11}$$

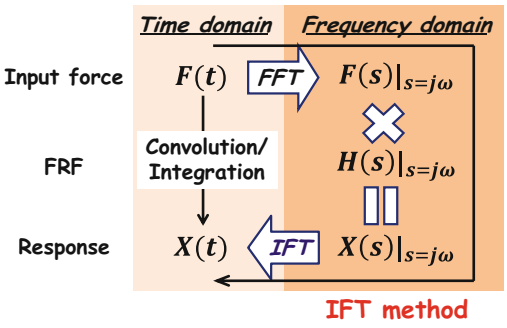

Fig. 13.3 Computation flow of IFT method

The velocity for the same time will also be calculated with the acceleration obtained and the initial condition for velocity as

$$\dot{p}_{t=i+1} = \{\dot{p}_{t=i}\} + (1-\beta)\,\Delta t\,\{\ddot{p}_{t=i}\} + \beta\Delta t\,\{\ddot{p}_{t=i+1}\} \tag{13.12}$$

Solving Eqs. 13.10, 13.11 and 13.12 repeatedly with the values obtained from these equations, the displacement, velocity and acceleration response will be obtained and the acceleration will be used for the SRS computation. The result of the Newmark solution depends on the constant factors such as the α, β and Δt. In this work, the α and β are set to 1/4 and 1/2 because the acceleration response for the system may be assumed to be constant for t = i and t = i + 1 [7]. The Δt is set to at least ten times smaller than the period of the highest frequency of interest to avoid numerical damping [5].

The modal acceleration responses obtained from the Newmark method will be transformed back to physical space using Eq. 13.3 and the number of modes used can be limited to the first set of M modes of the N possible modes for faster computation. The size of the mode shapes is also limited to M modes and then, the physical response with the limited number of modes will be obtained.

13.3.3 Time Response Computation with Frequency Response Function (FRF) in Frequency Domain

The time response computation in the frequency domain will also be calculated to compare the result with the Newmark method. Because the computation will be performed in the frequency domain, an input force needs to be transformed into the frequency domain using the Fast Fourier Transform (FFT) method and then a FRF will be multiplied by that spectrum. The result will be a response spectrum and a response time signal will be obtained from the IFT of this spectrum. The computation flow is summarized in Fig. 13.3 and the relationship between the input and output spectra is written as

$$X\,(\mathrm{s})\,\big|_{s=j\omega} = \mathrm{H}(s)\big|_{\,s=j\omega} \times F(s)\Big|_{s=j\omega} \tag{13.13}$$

Here, the FRF $\mathrm{H}(s)|_{s=j\omega}$ is obtained with the partial fraction form as

$$\mathrm{H}\,(\mathrm{s})\,\Big|_{s=j\omega} = \sum_{r=1}^{ndof}\left(\frac{q_r u_{jr} u_{kr}}{s-p_r} + \frac{q_r{}^* u_{jr}{}^* u_{kr}{}^*}{s-p_r{}^*}\right)\Bigg|_{s=j\omega}, \tag{13.14}$$

where $q_r = \frac{1}{2j\omega_r}$, $p_r = -\zeta_r\omega_r \pm i\,\omega_r\sqrt{1-\zeta^2}$ *and u is mode shape value of rth mode at j or k*

The input and output location are defined with the subscript *j* and *k* and the FRF will be calculated up to the Nyquist frequency, which is equal to Fs/2 Hz.

In order to obtain an acceleration spectrum from the result of Eq. 13.13, the displacement spectrum is scaled using

$$\ddot{X}(s)\,\big|_{s=j\omega} = -\omega^2 X(s)\big|_{\,s=j\omega} \tag{13.15}$$

For the acceleration spectrum obtained, the IFT will be applied and a response acceleration time signal will be achieved.

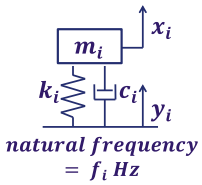

Fig. 13.4 SDOF model used in SRS calculation

The accuracy of this computation and the computation speed may depend on the frequency resolution of the spectrum or FRF. Each spectrum used in the frequency domain should have the same resolution to perform the multiplication of Eq. 13.13 and the frequency resolution can be written as

$$\Delta \mathrm{f} = \frac{F_s}{nfft}, \text{ where } F_s \text{ is sampling frequency and nfft is number of FFT points} \tag{13.16}$$

In order to make an easy comparison between the Newmark method and IFT method, the same sampling frequency as the Newmark method should be used for the IFT method because both of the results should have the same Δt, which is the time increment. If the time increment is set very small in the Newmark method, the sampling frequency of the IFT method will be large and the computation frequency range may be much wider than the frequency of interest. On the other hand, because the time response from this IFT method will have length of the number of FFT points (nfft), the nfft should be selected to the closest 2^n ($n = 1, 2, 3 \ldots$) considering the calculation steps of the Newmark method for faster computation.

13.3.4 Shock Response Spectrum (SRS)

The SRS can be obtained with a set of time responses excited by the shock input. An input shock may be measured data or a result of the FEA. Then, this shock will be treated as a base excitation and the upper SDOF structure will be anticipated to have a natural frequency of f_i Hz, which is shown in Fig. 13.4. The m_i, k_i and c_i represent mass value, stiffness value and damping value for the additional SDOF system in physical space. The m_i, k_i may vary based on the assumed natural frequency but the system is usually assumed to have a critical damping of 5 % (or some other prescribed constant value such as 1 or 2 %); this is generally due to the fact that the actual damping is not known before the structure is built. The input signal to the SDOF system is represented as y_i and the corresponding response is described as x_i. Basically, if an additional structure is attached to an arbitrary point of the base structure, the corresponding mass and stiffness of the base structure will be affected by the structural parameters of the additional structure. However, those are assumed to have negligible effect at the base structure in the SRS computation.

The SRS is always calculated only for a set of center frequencies of 1/6 or 1/12 octave band because any values in a particular band are assumed to have almost the same value. In this work, 1/12 octave band starting from approximately 1 Hz will be used for the SRS computation, which means the SRS will be calculated for a set of natural frequencies written as

$$\text{Center frequency } f_c = 1,000 \times 2^{\frac{1}{12}n} \text{ Hz, where n} = -120, \ldots, -1, 0, 1, 2, \ldots \tag{13.17}$$

The upper frequencies and lower frequencies for each octave band will also be described as

$$\text{Upper frequency } f_u = f_c \times 2^{\frac{1}{24}} \text{ Hz} \tag{13.18}$$

$$\text{Lower frequency } f_l = f_c / 2^{\frac{1}{24}} \text{ Hz} \tag{13.19}$$

This frequency band is determined based on the reference frequency of 1,000 Hz. The highest frequency of the octave band will be determined to one-eighth times of the sampling frequency to minimalize the potential computation error [6].

In order to obtain time responses for each SDOF system, the equation of motion for the SDOF model is written as

$$\mathrm{m}\ddot{x}_i = -c\left(\dot{x}_i - \dot{y}_i\right) - k\left(x_i - y_i\right) \tag{13.20}$$

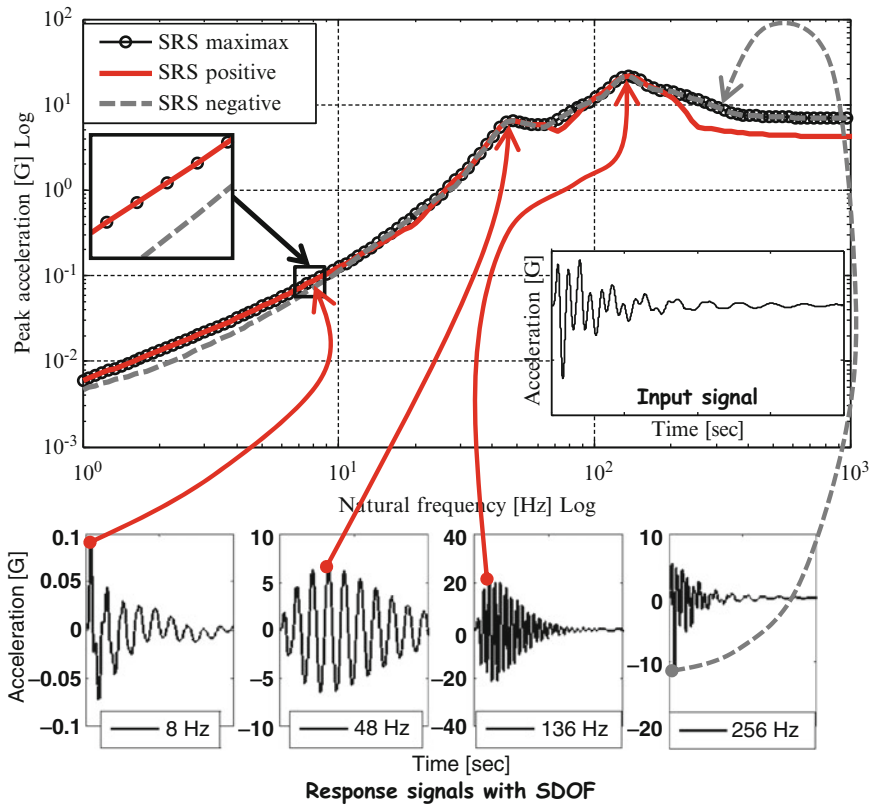

Fig. 13.5 Example of SRS computation

Then, $(x_i - y_i)$ can be re-written as z_i which represents the relative displacement. Using the z_i, Eq. 13.20 can be re-written to represent the relative response and its form is written as

$$\ddot{z} + 2\zeta\omega_n\dot{z} + {\omega_n}^2 z = -\ddot{y}(t),\ where\ \omega_n = \sqrt{\frac{k}{m}},\ \zeta = 5\ \% \tag{13.21}$$

The convolution integration approach will be used in Eq. 13.21 and the final form for the acceleration response is written as [6]

$$\begin{aligned}\ddot{x}_i &= 2\exp(-\zeta\omega_n\Delta t)\cos(\omega_d\Delta t)\,\ddot{x}_{i-1} - \exp(-2\zeta\omega_n\Delta t)\,\ddot{x}_{i-1} \\ &+2\zeta\omega_n\Delta t\,\ddot{y}_i + \omega_n\Delta t\ exp(-\zeta\omega_n\Delta t)\left\{\tfrac{\omega_n}{\omega_d}\left(1-2\zeta^2\right)\sin(\omega_d\Delta t) - 2\zeta\cos(\omega_d\Delta t)\right\}\ddot{y}_{i-1}, \\ &where\ \omega_d = \omega_n\sqrt{1-\zeta^2},\ \Delta t = \tfrac{1}{F_s} = time\ increment\end{aligned} \tag{13.22}$$

This equation will be applied to every natural frequency of interest which is defined in Eq. 13.17 and will be treated as a FIR filter applied to an input signal [6]. Then, a set of time responses will be obtained and in those signals, the maximum response value will be identified and plotted into the SRS. The procedure is shown schematically in Fig. 13.5. The lower four plots show examples for time responses caused by a shock input which is shown in the middle of Fig. 13.5. In those response signals, the maximum value will be picked up but the response acceleration may have its maximum value in positive or negative direction. In order to distinguish the effect of direction, there are two ways the SRS calculations are performed referred to as "Maximax SRS" and "Positive/ Negative SRS". The difference of these two methods is seen in Fig. 13.5. The Maximax SRS, which will be used in this work, is used to consider the absolute value of the response acceleration because the Maximax SRS will collect the maximum absolute value. On the other hand, the Positive or Negative SRS will pick up only for the positive maximum value or negative maximum value. They are used when an additional structure might have different endurance acceleration value for positive or negative direction.

13.3.5 Contribution Analysis and Mass Sensitivity Analysis (MSA)

In order to determine the effective location for mass modification, the MSA for the eigenvalues and FRF is widely used in field of modal analysis [8, 9]. Using these MSA, the most effective location to modify the natural frequency or amplitude of response vibration can be determined to meet the design. If the relationship between the modes and peaks of the SRS can be revealed by using the contribution analysis, these MSA will be useful to customize the envelope of the SRS.

Here, two ways computing the contribution analyses will be proposed. The first method is superimposing the FRF on SRS envelope. The FRF will be computed using Eq. 13.14 but the summation will not be performed in this case because the FRF for each mode needs to be plotted separately to make the contribution clearer. By comparing the peak of the FRF and the peak of the SRS, the contribution can be better understood. For example, if the FRF has a peak at a particular frequency and if the SRS has a peak at the same frequency, a mode existing at that frequency can be considered to have a significant contribution on the SRS, which means, in order to customize the SRS, the frequency and amplitude of that mode needs be customized. In the other case, if two or three modes exist in one octave band, all of these modes may need to be customized because these modes contribute to one peak of the SRS. The second method is the SRS computation with each modal response. If a set of SRSs are computed with each modal acceleration response scaled by mode shapes, each of these SRSs will show the contribution of each modal response on the envelope of the SRS. Superimposing these SRSs with modal response on the SRS with the original physical response, the contribution will be confirmed the same as the first method.

From the contribution analyses discussed above, an evaluation is needed to define which mode needs to be modified to obtain the desired SRS. And for the mode which is identified, two approaches for mass sensitivity analyses will be used to modify the contributions of the mode; the MSA for the eigenvalues and for FRF.

The MSA for the eigenvalues represents the sensitivity for eigenvalue modification [8]. The typical form of the equation of the eigensolution for each nDOF is written as

$$\left[[K] - {\omega_n}^2 [M]\right]\{X\} = \{0\}\,, \ \textit{where n is nDOF} \tag{13.23}$$

If a partial differential is applied to Eq. 13.23, the sensitivity for the eigenvalues will be obtained and its form can be written as

$$\frac{\partial \omega_n}{\partial \gamma_i} = \frac{1}{2\omega_n}\frac{\partial {\omega_n}^2}{\partial \gamma_i} = \frac{1}{2\omega_n}[U]^T\left[\frac{\partial [K]}{\partial \gamma_i} - {\omega_n}^2\frac{\partial [M]}{\partial \gamma_i}\right][U]\,, \ \textit{where n is nDOF and } \gamma_i \textit{ is design variable} \tag{13.24}$$

where design variable γ_i are composed only with mass number because only the mass modification will be conducted.

For example, if the mass sensitivity for the DOF 1 is required, the equation will be written as

$$\frac{\partial \omega_n}{\partial m_1} = \frac{1}{2\omega_n}[U]^T\begin{bmatrix} -{\omega_n}^2 & & & & \\ & 0 & & & \\ & & 0 & & \\ & & & 0 & \\ & & & & 0 \end{bmatrix}[U]\,, \ \textit{where n is nDOF} \tag{13.25}$$

This process will be done for every nDOF and each sensitivity value will be divided by the corresponding natural frequency in rad/s to regularize the values because sensitivity values of higher modes will always have higher values than the lower frequencies. Then, a sensitivity matrix with only negative values will be obtained because mass addition will lead to a decrease in the natural frequencies. The modification effect will be proportional to the modification value and, in order to increase the natural frequency, the mass value needs to be decreased.

Although the MSA for the eigenvalues can identify the effective mass location for eigenvalue modification, the sensitivity cannot estimate the behavior of the amplitude of the FRF, which means the FRF after the modification may have higher amplitude than the original one. To avoid this situation, the sensitivity analysis for the amplitude of FRF should also be considered in the customization process. The equation of motion shown in Eq. 13.1 is re-written as following in Laplace domain

$$\left[[M]s^2 + [C]s + [K]\right]\{X(s)\} = \{F(s)\} \tag{13.26}$$

Then, this equation can be transformed as

$$\{X(s)\} = \left[[M]s^2 + [C]s + [K]\right]^{-1}\{F(s)\} \tag{13.27}$$

When a unit input is applied to the DOF of the input location in the F(s), Eq. 13.27 will represent a Transfer Function for the system. Then, Eq. 13.27 will be transformed into the frequency domain and the sensitivity will be obtained by a partial differential of Eq. 13.27 as

$$\frac{\partial \mathrm{H(s)}\Big|_{s=j\omega}}{\partial \gamma_i} = \left\langle -\left[[M]s^2 + [C]s + [K]\right]^{-1}\left[\frac{\partial [M]}{\partial \gamma_i}s^2 + \frac{\partial [C]}{\partial \gamma_i}s + \frac{\partial [K]}{\partial \gamma_i}\right]\{H(s)\}\right\rangle\Big|_{s=j\omega}, \tag{13.28}$$

where design variable fl_i includes only mass for every nDOF

Because this sensitivity will be obtained as a series of complex numbers, these numbers need to be transformed into different levels for easier understanding of the sensitivity [9]. In addition, these sensitivity values in a particular octave bandwidth will be summed up to describe how each mass contribute to the SRS envelope; this is based on the estimation that, in order to reduce the amplitude of the SRS, all of the values of the FRF needs to have smaller amplitude in that octave band. In order to make a comparison of wide frequency easier, each summed value will be regularized with the maximum value of each mode because the sensitivity value in higher frequency will count values for wider frequency bandwidth than the lower frequency in the octave band. Due to this, the MSA for the amplitude of the FRF will have the maximum value of 1 or −1.

Comparing these two results of the sensitivity analyses, the effective mass location to obtain the desired SRS will be identified. If the contribution of the mode on the SRS is checked with the contribution analyses proposed, these sensitivities should have direct relationship with sensitivity for the SRS and should be useful for the SRS customization.

13.3.6 Structural Dynamics Modification (SDM)

The SDM [10] will be used to compute a response time signal for the modified system. The SDM can efficiently evaluate the modified response using the modal space representation for the system (either the original set of modes or the modified set of modes).

Using the SDM, the equation of motion for undamped system after the modification is written as[1,2]

$$\left[\begin{bmatrix}\ddots & & \\ & \overline{M_1} & \\ & & \ddots\end{bmatrix} + \left[\overline{M_{12}}\right]\right]\{\ddot{p}_1\} + \left[\begin{bmatrix}\ddots & & \\ & \overline{K_1} & \\ & & \ddots\end{bmatrix} + \left[\overline{K_{12}}\right]\right]\{p_1\} = 0, \tag{13.29}$$

$$\text{where } \left[\overline{M_{12}}\right] = [U_1]^T[\Delta M][U_1] \; and \; \left[\overline{K_{12}}\right] = [U_1]^T[\Delta K][U_1]$$

Here, $\left[\overline{M_{12}}\right]$ and $\left[\overline{K_{12}}\right]$ represent the modification effect in modal space. If the eigensolution is applied to Eq. 13.29, a set of new eigenvalues and eigenvector will be obtained. The eigenvalues from this solution represents a set of new natural frequencies for the modified system. The eigenvectors from Eq. 13.29 will provide

$$\{p_1\} = [U_{12}]\{p_2\} \tag{13.30}$$

With Eqs. 13.29 and 13.30, the equation of motion for the modified undamped system in modal space will be written as

[1]For the SDM, subscript 1 means parameter for the original model and subscript 2 means parameters for the modified model. In general, original structural and modal matrices will be presented without any subscripts.

[2]A term written in capital alphabet means matrix. A term with small alphabet means a component of matrix. For example, $\overline{M}$ means a modal mass matrix and $\overline{m}_i$ means a modal mass value for "i"th mode.

$$\begin{bmatrix} \ddots & & \\ & \overline{M_2} & \\ & & \ddots \end{bmatrix} \{\ddot{p}_2\} + \begin{bmatrix} \ddots & & \\ & \overline{K_2} & \\ & & \ddots \end{bmatrix} \{p_2\} = \{0\},$$
$$\text{where} \begin{bmatrix} \ddots & & \\ & \overline{M_2} & \\ & & \ddots \end{bmatrix} \rightarrow \begin{bmatrix} \ddots & & \\ & I & \\ & & \ddots \end{bmatrix} and \begin{bmatrix} \ddots & & \\ & \overline{K_2} & \\ & & \ddots \end{bmatrix} \rightarrow \begin{bmatrix} \ddots & & \\ & {\omega_2}^2 & \\ & & \ddots \end{bmatrix} \tag{13.31}$$

The modified modal damping matrix $\overline{C_2}$ can also be obtained using Eq. 13.7 with the modified modal mass and stiffness matrices. Using these modal parameters, the Newmark method or the IFT method will be performed to obtain a time response for the modified system. If the time response computation is conducted in modal space with the Newmark solution, the response signal will be transformed back into physical space using mode shapes for the modified system which is written as

$$\{X_2\} = [U_2]\{p_2\} = [U_1][U_{12}]\{p_2\} \tag{13.32}$$

This summarizes the major tools that are necessary for the analysis of the response for the SRS computations. The next sections cover the two example systems: a simple analytical 5-DOF system and a beam structure (both a finite element model and experimental configuration).

13.4 Analytical Example for 5-DOF System

13.4.1 Trial of the Methodology for Customizing SRS

In this section, the methodology proposed in this paper will be presented with a simple example of a 5-DOF system. The model used here and its structural parameters are shown in Fig. 13.6 with system data shown in Table 13.1. For this model, the modal solution will be applied and the acceleration response will be computed both in the time domain and the frequency domain using Eq. 13.11 or 13.13. These two responses from the Newmark method and IFT method will be treated as input signals for the SRS computation for the original system. Then, an arbitrary peak will be chosen to demonstrate the methodology for SRS customization. In order to modify the peak of the SRS, the mode contribution will be performed and the MSA will be applied to identify the most effective mass location for the modification. For this location, the SDM will be conducted and the modified acceleration response will be computed using Eq. 13.31 and Eq. 13.32. Finally, the SRS for the modified system will be computed and the effect of the modification will be judged comparing the difference in the SRS.

For the 5-DOF model, the physical mass and stiffness matrices are developed and the eigensolution will be performed using Eq. 13.2 with the results shown in Table 13.1. Using Eqs. 13.5, 13.6 and 13.7, the modal mass, stiffness and damping matrix will also be obtained assuming that the critical damping is 5 % for every mode.

In order to obtain the acceleration time response, an input force needs to be applied. For this study, a simple half sine pulse shown in Fig. 13.7 is used. Then, the Newmark solution is performed with the modal parameters obtained to compute the modal responses and all of the modal responses will be used to calculate the physical response shown in Fig. 13.8. The Newmark solution performs the time integration in every 2.441e−5 s for 0.2 s time duration. The time duration is determined

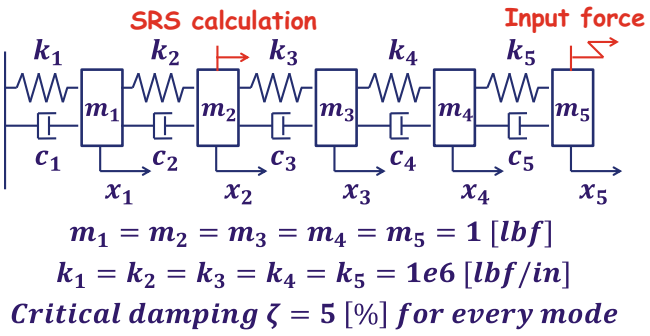

Fig. 13.6 5-DOF model used

Table 13.1 Parameters for each mode

Mode number	Natural frequency (Hz)	Mode shapes	Critical damping (%)
1st	45.30		5
2nd	132.23		5
3rd	208.45		5
4th	267.78		5
5th	305.42		5

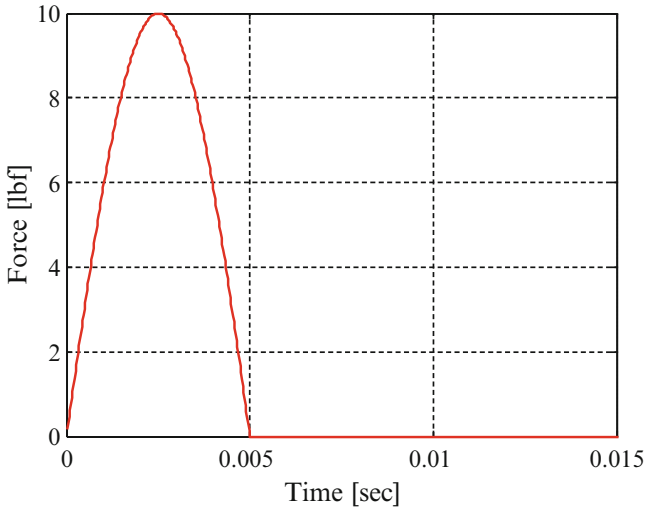

Fig. 13.7 Applied input force

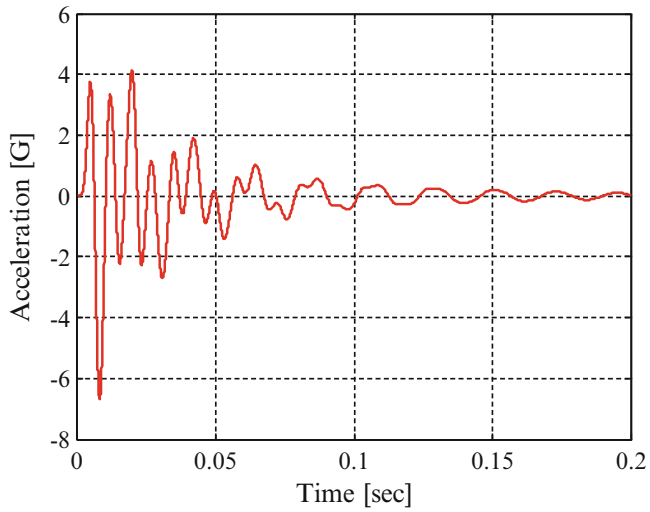

Fig. 13.8 Acceleration response with Newmark method

based on the damped response because the signal should be damped well in the time block to avoid the leakage error in the FFT or IFT. The valid upper frequency for this computation is considered as 4,096 Hz because the sampling frequency used is 40,960 Hz. Although this is much higher than the highest natural frequency of the system, the sampling frequency needs to be very high to allow small time increment to obtain the peak value in the resulting time signal correctly.

Because the time response will also be computed in the frequency domain, the input force will be transformed into the frequency domain using the FFT and the result is shown in Fig. 13.9. The nfft used is 131,072 and, with this value and the sampling frequency of 40,960 Hz, the frequency resolution for the spectrum will be 0.3125 Hz. Applying the modal parameters which are obtained from the eigensolution into Eq. 13.14, the FRF for the 5-DOF system can be obtained and is shown in Fig. 13.10 in terms of accelerance. With this FRF and the input spectrum obtained, the response spectrum will be calculated using Eq. 13.13. For the response spectrum obtained, IFT will be applied to obtain the time signal and the

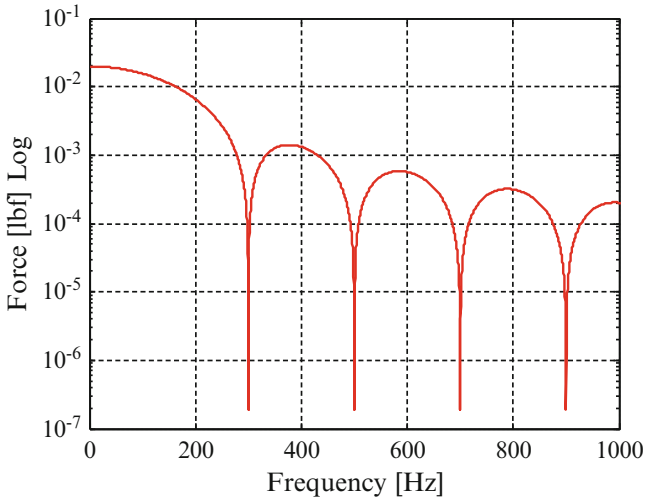

Fig. 13.9 Input force spectrum

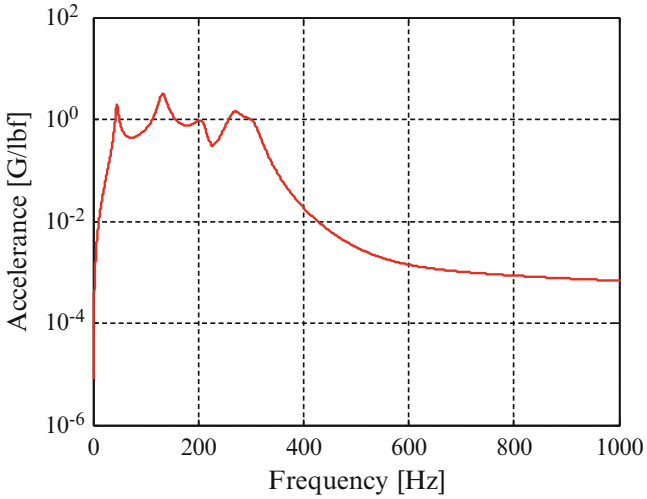

Fig. 13.10 FRF with modal solution

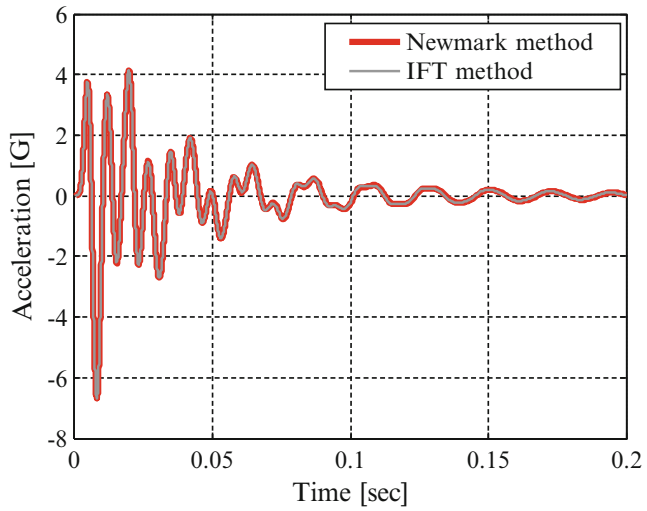

Fig. 13.11 Comparison of time response

response signal will originally have length of 131,072 but only the first $Fs \times 0.2$ set of data will be used. The result is shown in Fig. 13.11 and the time response with the Newmark method is overlaid. Both of the signals compare well with less than 0.2 % difference on the peak point.

Using the acceleration signals computed from the Newmark method or IFT method shown in Fig. 13.11, the SRS will be developed using 1/12 octave band shown in Eq. 13.17. For each additional SDOF system whose natural frequency is the

Fig. 13.12 Comparison of SRS

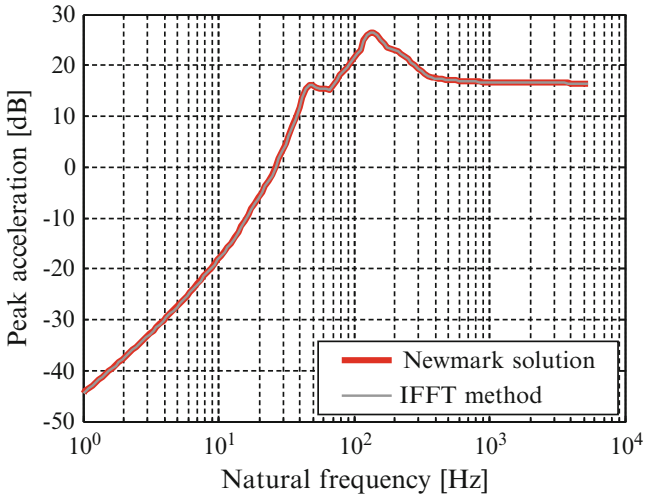

Fig. 13.13 FRF versus SRS

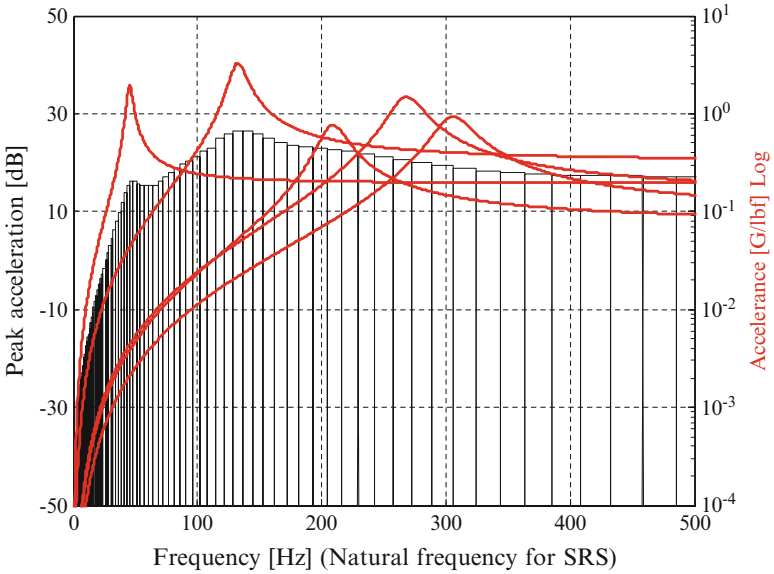

center frequency of the octave band, the maximum acceleration response value will be obtained with Eq. 13.22. The percent of critical damping of the SDOF system is assumed to be 5 %. Figure 13.12 shows the SRS developed with the time domain response and frequency domain response solution and the SRS is calculated up to one-eighth of the sampling frequency of the input signal, which is approximately 5,000 Hz. In this work, the SRS is plotted in decibel scaling with the reference value of 1 G; note that this value is different from the reference value defined in ISO 1683 [11]. Because both of SRSs shown in Fig. 13.12 provide almost the same result with less than 0.3 % difference in the maximum peak, both solutions in the time domain and frequency domain are considered to be useful for the SRS computation. However, the IFT method provides only the physical response and this is not convenient for entire flow of this work because the modal responses will be required to perform the contribution analysis. Due to this, the IFT method will be performed only for the comparison of the original SRS computation with the Newmark solution and will not be used for the SRS customization procedure.

The maximum peak on the SRS is found as a peak around 132 Hz. For the SRS customization procedure, this peak will be used for the demonstration of the methodology. In order to evaluate the relationship between the modes and peaks of the SRS, the contribution analysis will be performed in two ways: superimposing the FRF on the SRS or the SRS computation with modal response.

In Fig. 13.13, the FRF is superimposed on the SRS and the left Y-axis shows values of the SRS and the right Y-axis shows values of the FRF. The SRS is plotted in the form of bar graph because the relationship between a particular peak of the FRF and the value of a particular octave band will be obvious. From this result, each of the first and second modes is considered to have high contribution to each of the first and second peak of the SRS because the FRF has peaks close to the peak frequency

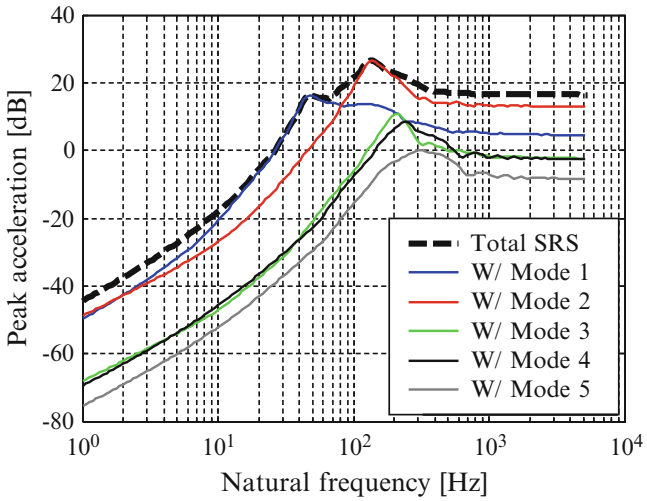

Fig. 13.14 SRS with modal response

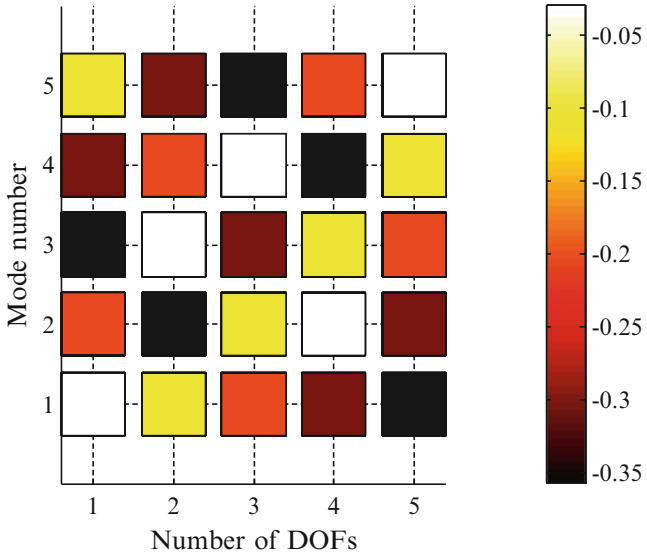

Fig. 13.15 MSA for the eigenvalues

of the SRS. However, the third, fourth and fifth modes are considered to have small contribution because there are no obvious peaks of the SRS near to the peaks of the FRF.

In Fig. 13.14, each modal response which is computed with the Newmark method is used for the SRS computation. These modal responses used are scaled by the mode shapes separately and each SRS obtained is influenced only by each mode. Here, the SRSs with the first and second modal response have approximately the same peak values as the original SRS at the first and second peak. However, the SRSs with the third, fourth and fifth modal response have smaller values than the original SRS. Due to this, the first and second modes are considered to have strong contribution to the SRS but the others do not.

As a result, the maximum peak of this SRS is considered as being influenced largely by the second mode of the system. Because these contribution analyses showed the second mode of the system contributes to the second peak of the SRS strongly, in order to identify the most effective location for the modification, the MSA will be applied to the 5-DOF system.

Using Eq. 13.24, the MSA for the eigenvalues will be obtained as shown in Fig. 13.15 and the X-axis represents the DOF of the system and the Y-axis represents the number of modes. From this result, the DOF 2 or 5 are considered to be useful to lower the natural frequency of the second mode. On the other hand, the DOF 4 is thought to have small effect for eigenvalue modification because the DOF 4 is a node of the mode.

In addition, in order to identify the most effective location to decrease the amplitude of the FRF, the MSA for FRF will also be performed using Eq. 13.28. In this case, the MSA for FRF is summed up with bandwidths of seven octave bands each of which have the peak octave band at the middle, which means the result will show the sensitivity of amplitude reduction in those octave band entirely and which describes the effectiveness of the locations to modify each peak of the SRS. The

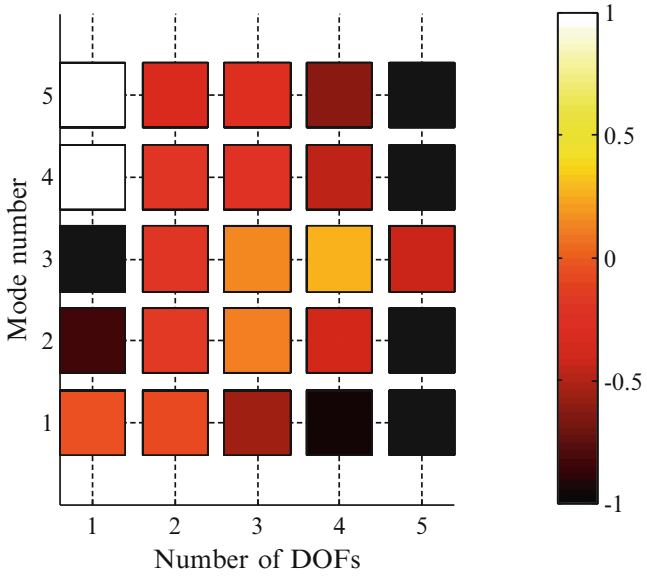

Fig. 13.16 MSA for FRF

Table 13.2 Comparison of natural frequencies

	Natural frequency (Hz)		
Mode number	Original	Modified	Diff. (%)
1st	45.30	41.55	−9.02
2nd	132.23	124.23	−6.44
3rd	208.45	200.99	−3.71
4th	267.78	263.49	−1.63
5th	305.42	304.20	−0.40

result is shown in Fig. 13.16 and the DOF 5 is considered to be effective for lowering the amplitude of the second mode because of the maximum sensitivity. If the MSA for FRF outputs positive values such as that for mode number 4 or 5 for the modification of DOF 1, the FRF modified will have higher amplitude in those defined frequency bandwidth.

If the goal of the modification is lowering the natural frequency and reducing amplitude of the FRF, then DOF 5 can be considered to be proper for the modification because this location has high sensitivity values for both sensitivity analyses.

In order to customize the second peak of the SRS, the SDM will be performed by increasing the mass value of the DOF 5 by + 50 % from the original model to check the effect. From Eq. 13.31, the natural frequency for the modified system will be achieved and, in Table 13.2, these values are shown with comparison of the original values. From this result, the natural frequency of the second mode is confirmed to be decreased from the original value.

In order to verify the change in the FRF, the original and modified FRF are superimposed in Fig. 13.17. Here, the modified FRF is computed using Eq. 13.14 with the modified modal parameters obtained from the SDM and a reference solution which is performing a modal solution directly on the modified system. These two modified FRFs are the same and have smaller amplitude at the second mode than the original FRF. Using the same set of modal parameters used for the FRF computation, the modified time response can be calculated with the Newmark method in modal space. The modified physical response from the SDM and the reference solution is shown in Fig. 13.18 and compared to the original response and two of the modified responses compare well. These accelerations are used for the SRS computation and the result is shown in Fig. 13.19. The modified SRS has smaller amplitude for the second peak and the peak frequency is shifted lower. The maximum peak frequency is shifted by 7 Hz and its amplitude is decreased by 3 dB. The modified SRSs with the SDM and the reference solution are the same because the signals used for the calculation are also the same. Due to this, the effect of the SRS modification can be measured with the modified response using the SDM procedure.

Although these figures showed good results and the modified SRS achieved the goal defined, the mass location of the modification may not be the best because the modification was attempted only for one location. In order to confirm the methodology, the same SDM procedure will be applied to every DOF and the modification value is consistently set to +50 %. Figure 13.20 shows the result and the DOF 5 is confirmed to have the smallest amplitude for the second peak of the FRF with the biggest frequency shift in these five patterns. Due to this, the methodology for customizing the SRS to meet the design is considered to be appropriate. In addition, the modification effect will be checked using various modification

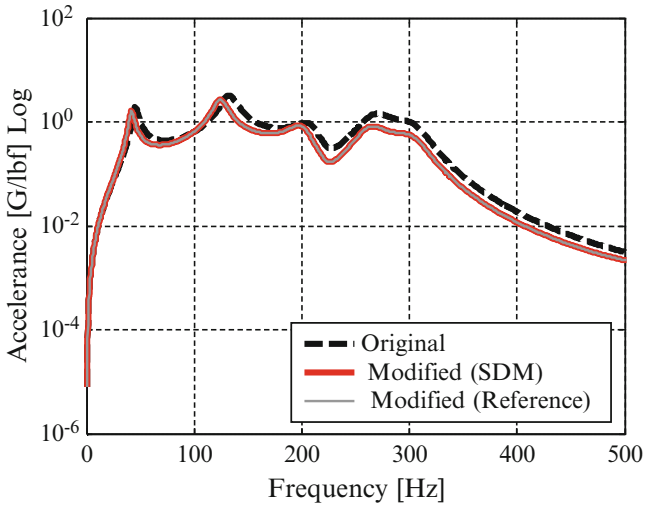

Fig. 13.17 Comparison of FRF

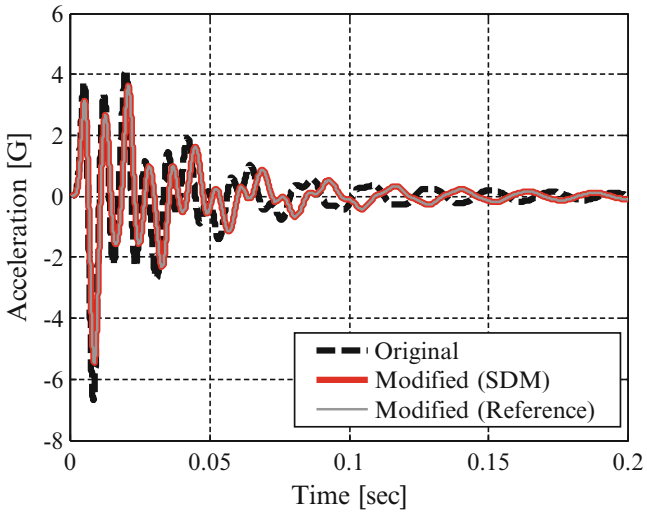

Fig. 13.18 Comparison of time signal

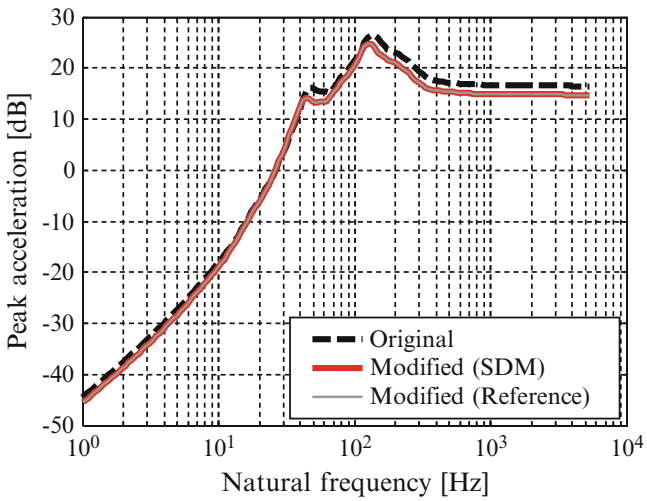

Fig. 13.19 Comparison of SRS

values for the best modification location of the DOF 5. Figure 13.21 shows the result for four different modification values: +10, +30, +50 and +100 %. From this result, the modification effect on the SRS is confirmed to be proportional to the modification value. If the value is modified significantly, the SRS will also be modified significantly but the modification value should be determined in a feasible range because +100 % modification may not be realistic for an actual design.

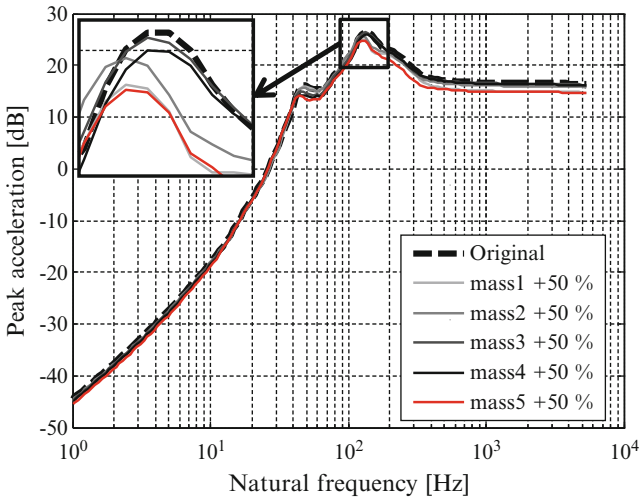

Fig. 13.20 Effect of modification location

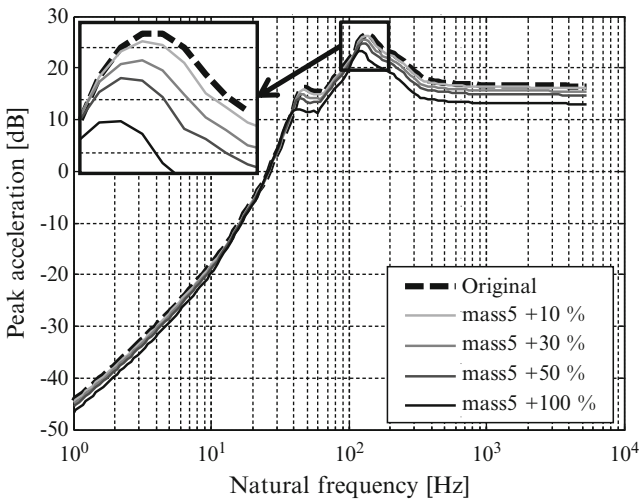

Fig. 13.21 Effect of modification value

13.4.2 Proper Configurations for SRS Computation

Here, the following three configurations will be discussed for the proper SRS computation: the time duration of the input signal used for the SRS computation, the sampling frequency for that time signal, the number of modes used for the time signal computation.

The SRS developed in the previous section uses the acceleration signal with 0.2 s duration for its development. Because the specification of some frequency components may not clearly appear in a shorter time window, five different time lengths will be used for the discussion: 0.01, 0.05, 0.1, 0.2 and 0.5 s. The sampling frequency is set to 40,960 Hz and all of the modes are used for the time response computation with the Newmark method. Figure 13.22a shows the difference of the time signals and within approximately 0.2 s, the signal is considered to be damped well. Figure 13.22b shows a comparison of the SRSs computed with these five signals. From this result, if the signal for the SRS computation is too short like 0.01 s, which is just twice the input pulse duration, the SRS obtained will have different envelope from others because the each modal response has not achieved their maximum response. On the other hand, if a signal used for the SRS is long enough such as 0.1, 0.2 or 0.5 s, the response signal is considered to be adequate to collect the maximum response value to compose the envelope of the SRS because the peak specifications of the SRS are the same for these time signals. Due to this, the signal used for the computation needs to be long enough to collect the maximum response values but does not necessarily need to be damped well in the time span to estimate the peak values from the development of the SRS.

The sampling frequency will affect not only the upper frequency limit of the SRS computation but the peak values of the SRS because the acceleration time signal may have different peak values based on the time increment of the Newmark method if the sampling frequency is low. Here, some sampling frequencies will be used to discuss the effect; 2,560, 5,120, 10,240, 20,480 and 40,960 Hz. Time length of input signal is set to 0.2 s because 0.2 s signal was considered to be long

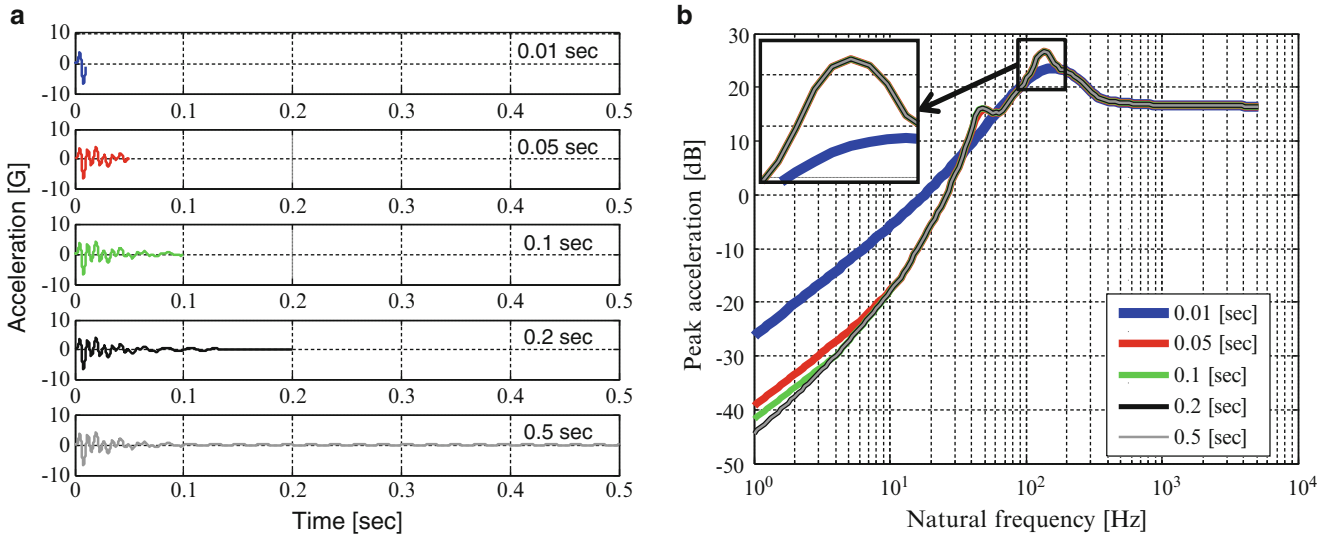

Fig. 13.22 Effect of input time length (**a**) acceleration signal, (**b**) SRS comparison

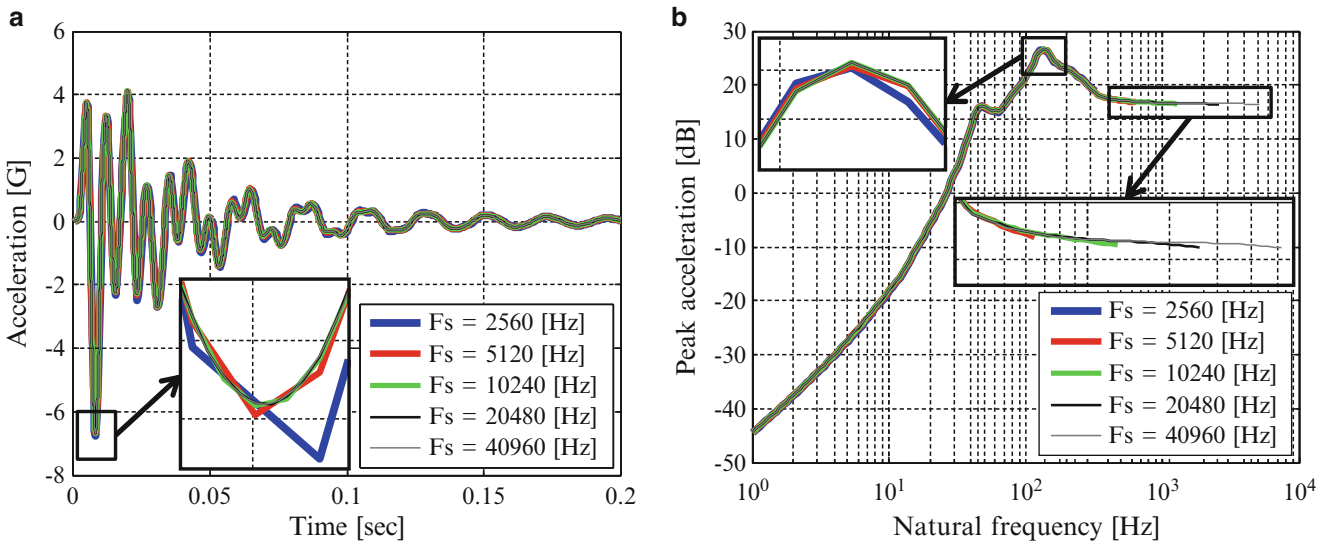

Fig. 13.23 Effect of sampling frequency (**a**) acceleration signal, (**b**) SRS comparison

enough for this study from the previous section and all modes are used for physical response computation. Figure 13.23a shows the effect of different sampling frequencies and there are some differences seen at some peaks as discussed above. This is because a signal with high sampling frequency has smaller time increment and high number of data points so the peak values are identified well. However, for the SRS shown in Fig. 13.23b, all of the signals have almost the same value. Because the SRS computation is done in every octave band, slight difference in amplitude or frequency of the input signal may not be so important for the SRS computation. As a result, although the sampling frequency does not affect the peak values of the SRS that much, the value should be high enough to reproduce a peak value in the time domain well and should be determined based on the upper limit of the frequency of interest.

This work uses the physical acceleration with the modal superposition techniques for the SRS computation if the computation is performed in the time domain. Here, the number of modes can be limited for faster computation. Although the computation will be faster if small number of modes is used, specification of the SRS may degrade. In order to check this effect, the number of modes used for the computation will be changed; only the first mode, first two modes, first three modes, first four modes and all modes. The time length and sampling frequency are set to 0.2 s and 40,960 Hz based on the previous considerations. Figure 13.24a shows a comparison of acceleration signals and these signals are used for the SRS computation. Figure 13.24b shows a comparison of the SRS. Of course, if a large number of modes is used for the

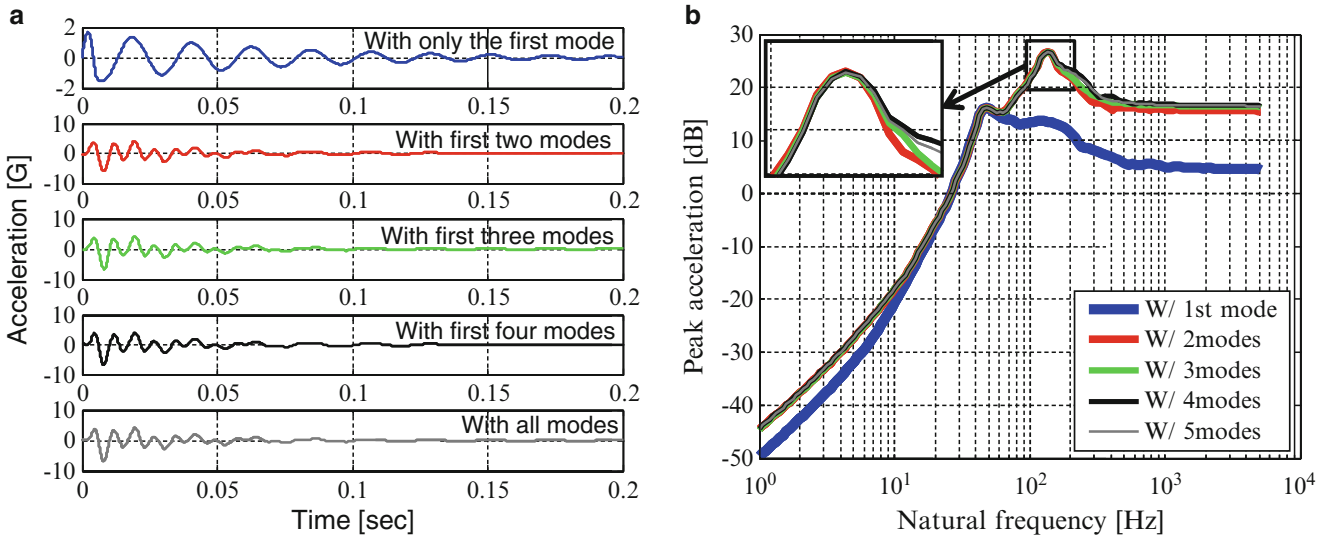

Fig. 13.24 Effect of number of modes (**a**) acceleration signal, (**b**) SRS comparison

computation, a more correct SRS will be obtained but the maximum peak value of the SRS can be estimated with the limited number of modes if the modal response which may cause the maximum response is included. For example, if the second peak of the SRS is dominant and if the second mode contributes to the peak well, the SRS calculated with the first two modes is enough to evaluate the maximum peak value.

13.5 Analytical/Experimental Example for Beam Structure

13.5.1 Experimental SRS Measurement/EMA for Acquiring Modal Parameter

For the studies performed here, a beam shown in Fig. 13.25 will be used to evaluate the methodology. The beam which has cross section of 2 in. by 1 in. with 6 ft length is suspended on the upper end of the beam to simulate free-free configuration. Free-free configuration is chosen because of its simplicity in the boundary condition. This beam is made of aluminum and the surface is covered with duct tape to provide some damping. An input force is applied to the lower end of the beam #19 and the SRS will be developed at the location of #8 which is 28 in. away from the upper end. For constant input, a pendulum shown in Fig. 13.25 is utilized and a load cell is introduced to the weight of the pendulum to measure the input signal and a soft tip is attached on the load cell. In order to measure the acceleration signal, an accelerometer is located to the location of #8.

For a proper experimental SRS measurement, some configurations including the measurement time duration, the sampling frequency and the number of modes used for signal computation need to be determined. Although the sampling frequency may affect the peak value of SRS and will limit the upper frequency, the sampling frequency is set to 40,960 Hz because this value will provide a small enough time increment and the computation time may be long if higher sampling frequency is used. Here, the acceleration signals with four different time lengths will be measured: 1.6, 4.0, 8.0 and 16 s time duration. Figure 13.26 shows the difference in the input time signals used for these four measurements and the pendulum is confirmed to produce essentially the same input consistently with less than 2 % difference in the peak value. These input signals cause the acceleration response at the output location and Fig. 13.27 shows the measured acceleration responses. Because the input signals have similar envelope and amplitude, the output signals also have high similarity. Using these acceleration signals, the experimental SRSs are developed using Eq. 13.22 and Fig. 13.28 shows the result. From this result, the SRS with the 1.6 s time duration signal is different from others in low frequency but all of them except for 1.6 s have high similarity for every peak of their SRS in high frequency. Due to this, the acceleration signal with 4.0 s length is considered to be long enough for the SRS computation for this case. Although the signal with 4.0 s duration is not damped well in its time duration, the SRS with 4.0 s signal has high similarity as SRSs with longer time duration because the maximum response values caused by the input signal are obtained in that duration. Furthermore, because the peak values of these four SRSs are almost the same, the input forces with less than 2 % difference are considered to be sufficient for measuring the effect of the modification. For the

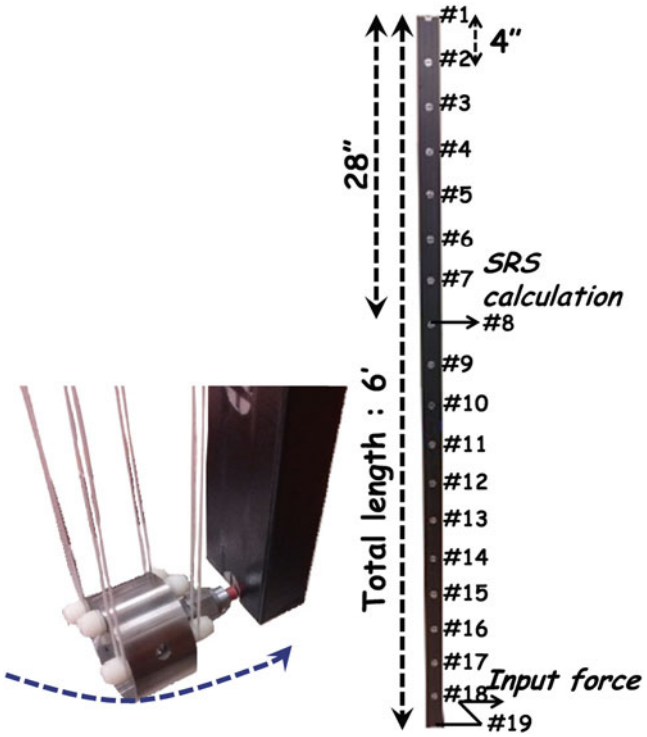

Fig. 13.25 Measurement setup

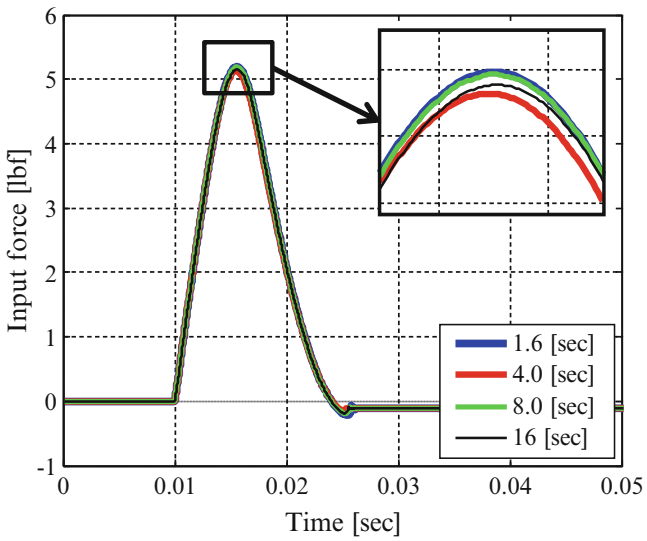

Fig. 13.26 Input signal comparison

customization procedure, the biggest peak near 40 Hz will be used. The frequency of interest can be set as up to 2 kHz based on the envelope of the SRS and the physical response will be calculated with modes existing lower than 2 kHz.

Based on the frequency range of interest determined, the EMA will be conducted to develop a proper experimental or analytical model. Using three kinds of modal impact hammers, a set of FRFs will be measured to estimate the mode shapes, natural frequencies and dampings. The following three different configurations will be used for the EMA.

Configuration (i): Fs = 512 Hz, nfft: 32,768, $\triangle$f = 0.016 Hz, T = 64.0 s
Configuration (ii): Fs = 1,280 Hz, nfft = 32,768, $\triangle$f = 0.039 Hz, T = 25.6 s
Configuration (iii): Fs = 5,120 Hz, nfft = 32,768, $\triangle$f = 0.156 Hz, T = 6.4 s
(Fs: sampling frequency, $\triangle$f: frequency resolution, T: acquisition time)

These configurations are determined based on the estimation that lower modes might have low damping. Because a proper damping value is required for better SRS computation and applying any windows is not proper for better damping value estimation, the signal needs to be decayed well within the acquisition time to avoid the leakage error. The examples of the input forces and modal hammers used are shown in Fig. 13.29. With these hammers, the input forces will be added

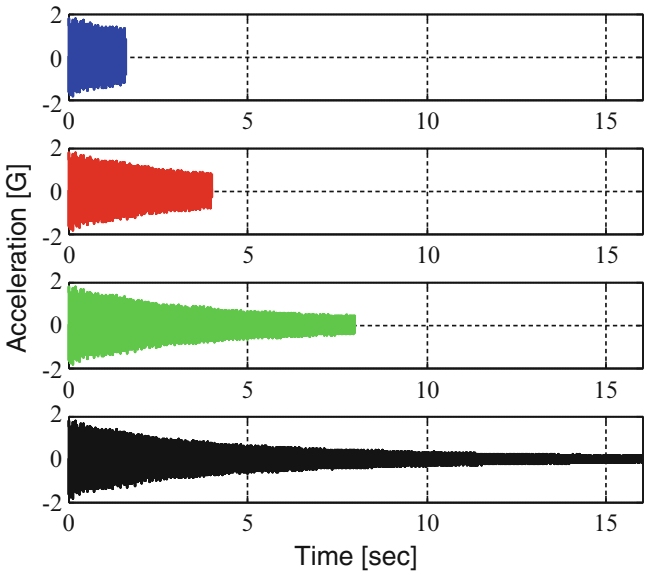

Fig. 13.27 Output signal comparison

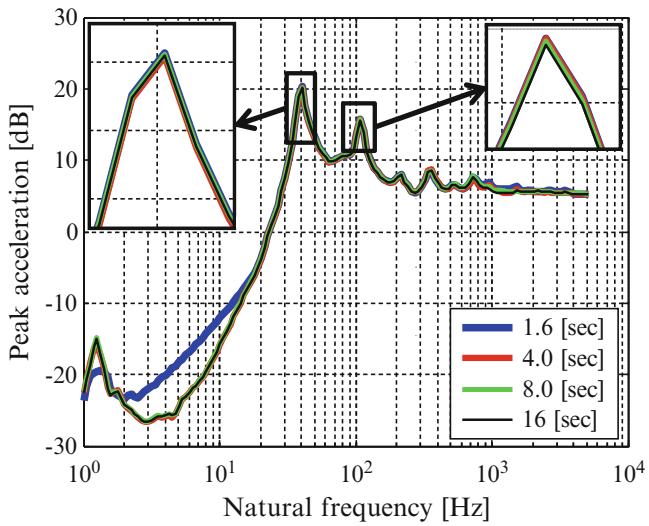

Fig. 13.28 SRS with various time spans

to all of the locations starting from #1 to #19. An accelerometer is consistently placed at the location #8 to measure the response acceleration and then, 19 sets of FRFs will be obtained with the three different configurations. Figure 13.30 shows the example of the FRFs measured with these three configurations between the input location #19 and the output location #8. Due to the leakage error depending on the short acquisition time, modal parameters of the first few modes are hard to estimate from the FRF shown in Fig. 13.30c which is measured with the configuration (iii). On the other hand, using a proper configuration, which is configuration (i), these modal parameters for the first few modes can be measured from the FRF shown in Fig. 13.30a. The first two rigid-body modes and two bending modes will be extracted from the FRF with the configuration (i) and the next three bending modes will be extracted with the configuration (ii) and for the other modes exist lower than 2 kHz, the configuration (iii) will be used. Table 13.3 shows the results of the EMA and the frequencies, damping and some examples of mode shapes are shown. Applying these parameters into Eqs. 13.5, 13.6 and 13.7, the modal mass, stiffness and damping matrices will be developed and the equation of motion will be developed experimentally. Figure 13.31 shows the FRF computed with these data using Eq. 13.14 compared to the measured FRF with the configuration (iii). This FRF will be called the synthesized FRF and this FRF will be used for the discussion of the contribution analysis and the SDM. The measured FRF has torsional modes at some frequencies but the synthesized does not because the modal parameters are extracted only for bending modes.

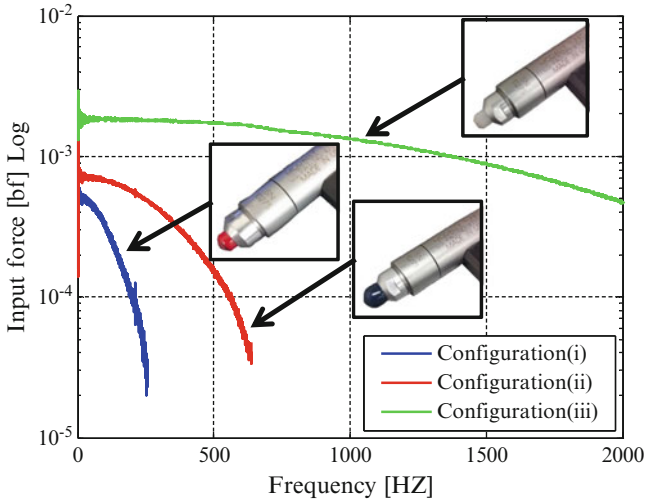

Fig. 13.29 Example of input forces

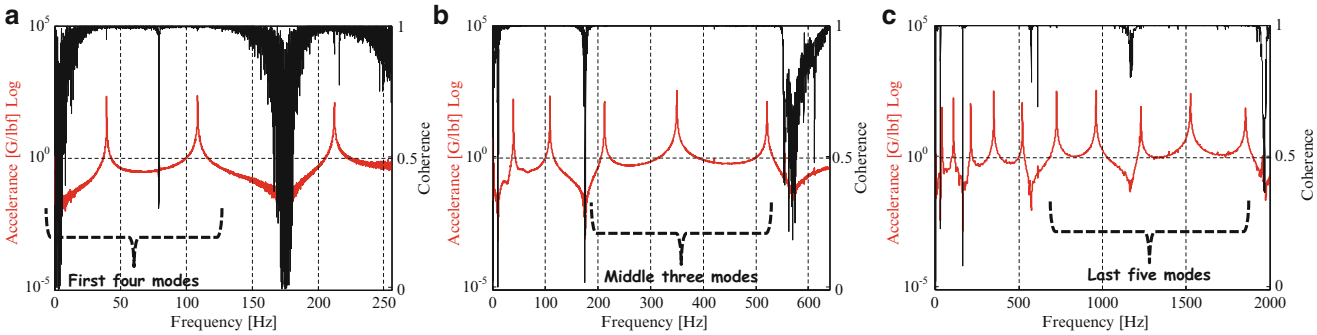

Fig. 13.30 Comparison of measured FRFs (**a**) FRF with configuration (i), (**b**) FRF with configuration (ii), (**c**) FRF with configuration (iii)

Table 13.3 Results of EMA

Mode #	Mode name	Natural frequency [Hz]	Mode shapes	Damping [%]
1	1st rigid-body	1.251		0.2309
2	2nd rigid-body	1.713		1.0244
3	1st bending	39.437		0.0272
4	2nd bending	108.478		0.0259
5	3rd bending	212.418		0.0283
6	4th bending	349.881		0.0260
7	5th bending	521.407		0.0209
8	6th bending	725.244		0.0193
9	7th bending	961.455		0.0232
10	8th bending	1230.080		0.0319
11	9th bending	1525.900		0.0346
12	10th bending	1855.130		0.0523

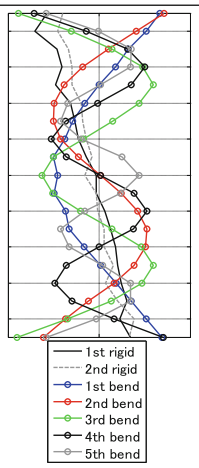

13.5.2 FE Model Development Using Measured Modal Parameters

In order to calculate a SRS from the FEA and compare the SRS with the one from the experiment or the EMA, an FE model will be developed to simulate the experimental model as shown in Fig. 13.32. The mass and stiffness matrices were developed using planar beam theory. The beam is made of aluminum, the mass density is 2.588e−4, the Young's modulus E is 10e6 psi and the moment of inertia $I = \frac{ab^3}{12}$ is 6.510e−4 in ˆ3 considering the rectangular cross section. The beam model is

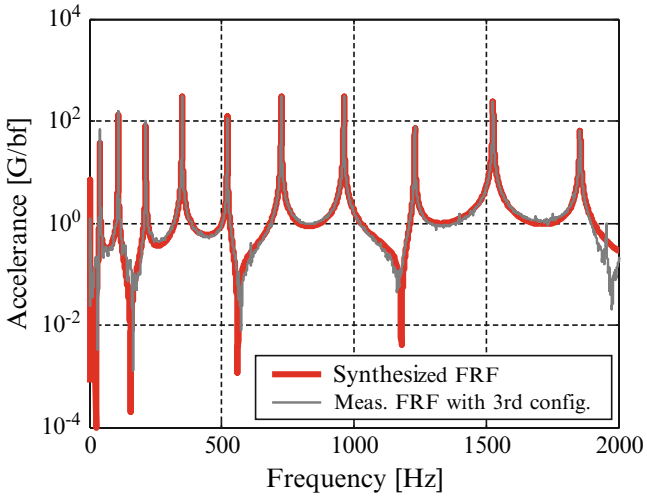

Fig. 13.31 Synthesized FRF by EMA

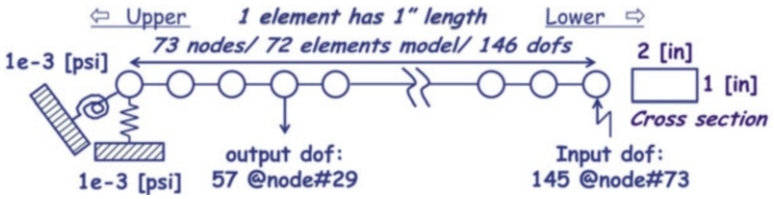

Fig. 13.32 FEA model

Table 13.4 Comparison of eigenvalues

Mode #	Mode name	Natural frequency (Hz)		Diff. (%)
		EMA	FEA	
1	1st rigid-body	1.251	0.0033	−3.78E+4
2	2nd rigid-body	1.713	0.0522	−3.18E+3
3	1st bending	39.437	38.98	−1.17
4	2nd bending	108.478	107.44	−0.97
5	3rd bending	212.418	210.63	−0.85
6	4th bending	349.881	348.18	−0.49
7	5th bending	521.407	520.13	−0.25
8	6th bending	725.244	726.46	0.17
9	7th bending	961.455	967.18	0.59
10	8th bending	1, 230.080	1, 242.30	0.98
11	9th bending	1, 525.900	1, 551.81	1.64
12	10th bending	1, 855.130	1, 895.72	2.14

evaluated in a free-free condition with very soft end springs. For the mass and stiffness matrices developed, an eigensolution is performed and these eigenvalues obtained are shown in Table 13.4 with comparison of the EMA data and the flexible mode natural frequencies are in very good agreement. The mode shapes from the FEA are shown in Fig. 13.33. The mode shapes from the EMA and FEA are compared using the Modal Assurance Criteria (MAC) given as

$$MAC_{ij} = \frac{\left(\{U_i\}^T\{U_j\}\right)^2}{\left(\{U_i\}^T\{U_i\}\right)\left(\{U_j\}^T\{U_j\}\right)}, \text{ where } U_i \text{ and } U_j \text{ represent mode shapes at } j \text{ or } k \tag{13.33}$$

All the vectors are very well correlated as seen in Fig. 13.34 except for the rigid body modes which are not of importance for the studies here. Using Eqs. 13.5 and 13.6, the modal mass and stiffness matrices will be computed from the FEA and, for modal damping matrix, the modal damping values measured in the EMA, which is shown in Table 13.3, will be used with Eq. 13.7. With these matrices, the equation of motion in modal space will be developed and the FRF will also be calculated. Figure 13.35 shows the comparison of the FRFs obtained from the EMA and FEA. These results are similar because the natural frequency and mode shapes of both models are very similar and the measured damping values are used for both computations. These FRFs will be used to compute a time response with the IFT method and used to compare the effect of the modification.

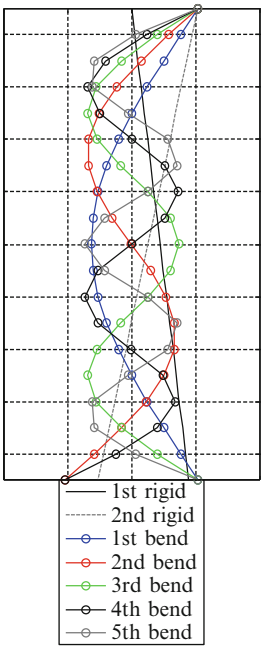

Fig. 13.33 Mode shapes (FEA)

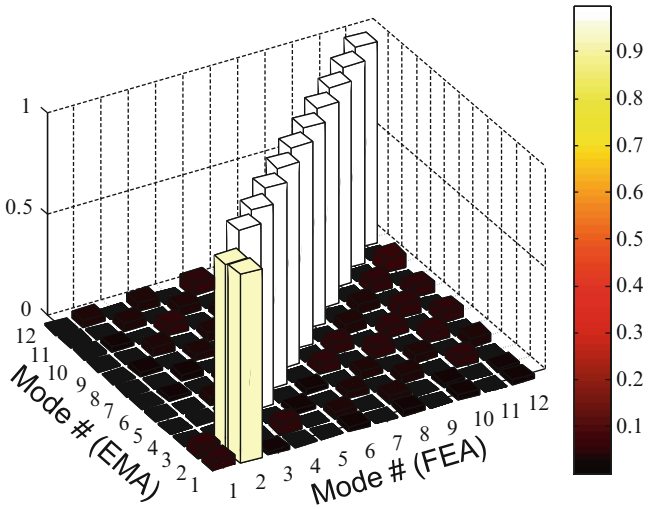

Fig. 13.34 MAC (FEA versus EMA)

13.5.3 SRS Computation with Time Response from Measured Data/EMA/FEA

With the modal parameters obtained from the EMA or FEA, an acceleration time response can be computed. The input force used for the computation is determined from the measured input force signal. This signal is measured with the sampling frequency of 40960 Hz and the envelope is shown in Fig. 13.36. This signal is the same as the one shown in Fig. 13.26, which is for the configuration of 4.0 s measurement. Then, the Newmark method or IFT method can be applied to the equation of motion in modal space which is obtained from the EMA and FEA.

Using the Newmark method, the modal responses will be computed first and then transformed into physical space using mode shapes obtained from the EMA and FEA. Here, the acceleration signals for the first 12 modes will be used for the computation because these modes are considered to be sufficient for estimating the peak values of the SRS and the modal parameters for the first 12 modes are extracted from the EMA. The sampling frequency for the Newmark method is set as 40,960 Hz; the upper frequency of interest is 2 kHz but the small time increment is needed to assure that accurate time response is obtained.

On the other hand, for the IFT method, the FRF will be constructed with 40,960 Hz sampling frequency and the nfft of 262,144. The frequency resolution for the spectrum will be 0.15625 Hz and the response signal will have the time length of the nfft but the signal for the first $Fs \times 4.0$ set of data will be used. The FRF which will be used for this computation was shown in Fig. 13.35 and the response time signal will be affected by the first 12 modes.

Fig. 13.35 FRF comparison

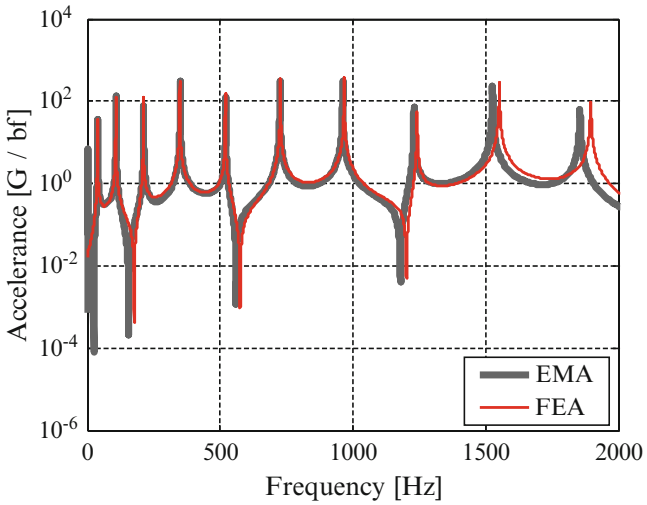

Fig. 13.36 Input force signal

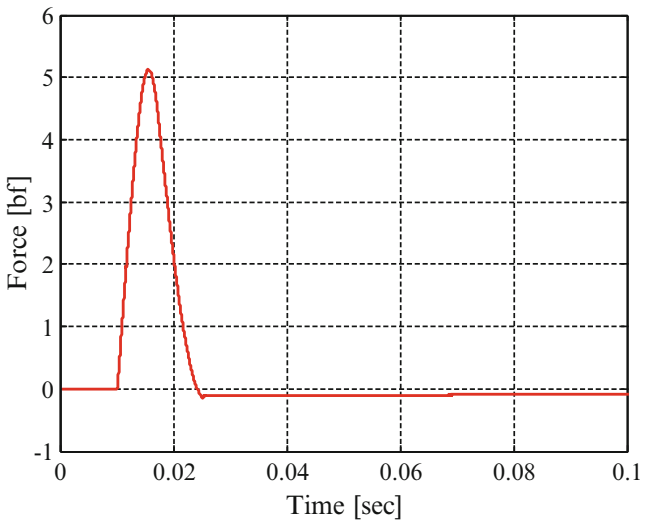

Figure 13.37 shows the comparison of the measured acceleration signal, results of the Newmark method and results of the IFT method. For the Newmark method and IFT method, time responses from the EMA and FEA are compared and all of the computed signals have almost the same response as the measured signal. Because the natural frequency and mode shapes of both solutions compare well and the measured damping values are used, the true signal is reproduced well as expected. However, the IFT method has slightly smaller amplitude than the Newmark solution and several reasons may explain why. First, the sampling frequency may not be small enough to accurately capture the peak time response. Second, the signal may suffer from slight leakage errors due to the overall sample period.

Finally, these signals will be used for the SRS computation and Fig. 13.38 shows the result. Compared to the SRS with the measured data, the SRSs with the Newmark method are very similar. Although the SRS with the IFT method is not different, the SRS with IFT method has slightly smaller value than the measured SRS or the SRS with the Newmark method because of the difference in amplitude of the time response signal. In addition, the SRS with the EMA data has smaller amplitude than the SRS with the FEA because of the same reason. Because the SRSs from the FEA are similar to the measured SRS, the SRS with the FEA data is considered to simulate the actual system well. Due to this, if the data from the EMA and FEA compare well and if the measured damping is used, the envelope of the SRS can be the same as the actual SRS and the first goal of this paper is achieved: the development of a correct solution for the SRS simulation.

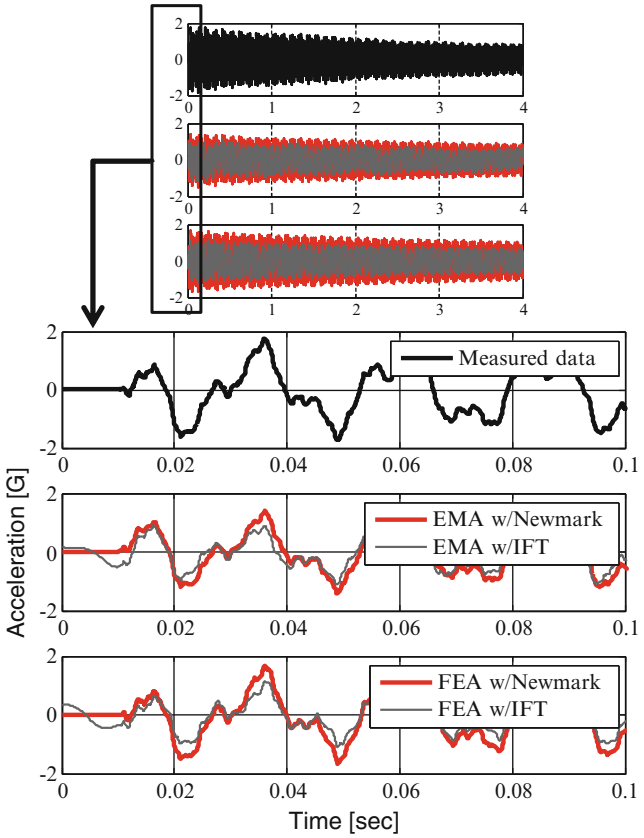

Fig. 13.37 Comparison of measured/calculated acceleration signals

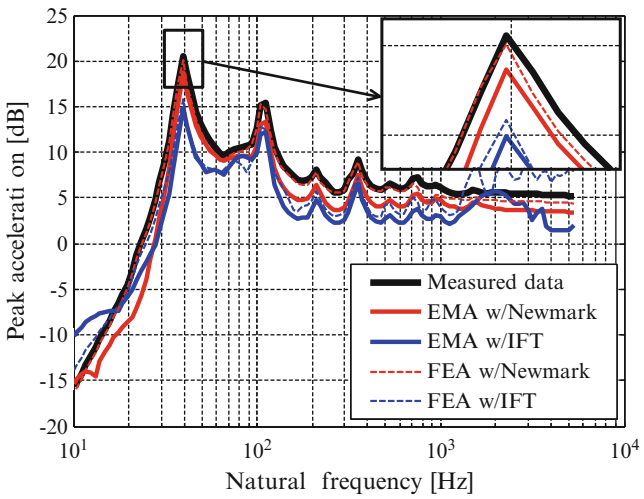

Fig. 13.38 Comparison of SRS from experiment/EMA/FEA

13.5.4 Trial of the Methodology for Customizing SRS

Here, the methodology proposed in this paper will be applied to the developed model. Using the SRS and modal parameters obtained from the EMA or FEA, the contribution of modes, MSA and SDM will be performed.

In order to clarify the relationship between the modes and peaks of the SRS, the contribution analysis will be performed. Here, a pair of SRSs which are developed from both the EMA and FEA will be used for the discussion. In Fig. 13.39, the FRFs computed from the EMA and FEA are superimposed on the corresponding SRSs. These SRSs are developed with the acceleration signals calculated with the modal parameters identified using the Newmark method. Here, the first four modal parameters of flexible modes are used to synthesize the FRF and the contribution is analyzed. From this result, the first and second modes of the beam are considered to have high contribution on the peaks of the SRS because the obvious peaks exist

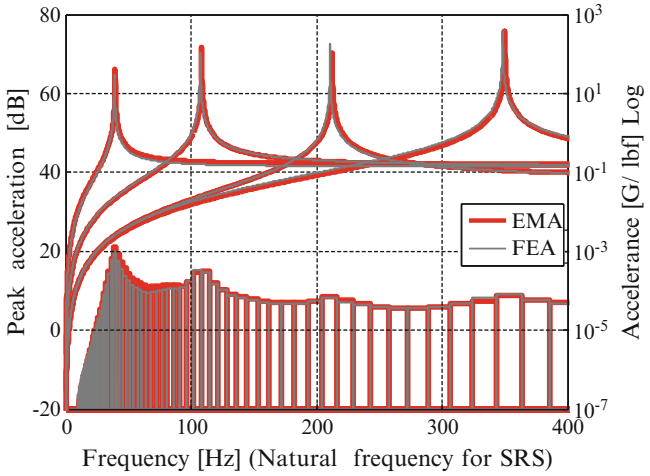

Fig. 13.39 SRS versus FRF

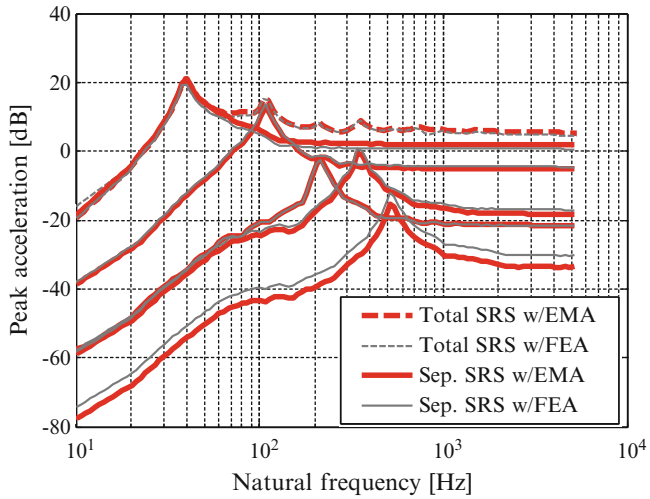

Fig. 13.40 SRS with modal response

at the same frequency. For the peak of the SRS to be modified, which is a peak around 40 Hz, the first bending mode of the beam is considered to have large contribution to the peak of the SRS based on this analysis. The contribution can also be estimated from the separate SRSs developed with each modal acceleration response. Figure 13.40 shows the result and, for the modal acceleration computation, the first five modes are used to analyze the contribution. From this result, the same as the result discussed previously, the first and second modes are considered to have high contribution and the first bending mode can be judged as the most dominant for the biggest peak of the SRS.

Due to this, the first mode of the beam will be customized to obtain the desired SRS. In addition, because there is only really small difference between two solutions from the EMA and FEA, this contribution analysis can be performed with just the FEA because both data sets are similar.

In order to customize the maximum peak of the SRS, for the first bending mode of the beam, the MSA will be applied to identify the most effective location for the mass modification. The goal of this modification is defined as lowering the peak frequency and decreasing the amplitude at the peak. Using Eq. 13.24, the MSA for the eigenvalues can be obtained and the result is shown in Fig. 13.41. Although the modal parameters extracted from the EMA can also be used but for this computation, only the modal parameters obtained from the FEA are used and the number of nodes is limited to have the same nodes as the experiment. The computation is done only for the bending mode because the modal parameters of the FEA are very similar to the EMA data only for the first ten bending modes. From this result, both of the ends of the beam are considered to have high sensitivity for the eigenvalue modification for the first bending mode. In addition, the MSA for FRF can be obtained using Eq. 13.28 and the result for the first ten bending modes is shown in Fig. 13.42. The sensitivity values are summed up with bandwidths of seven octave bands each having the peak octave band in the middle. From this result, both ends of the beam are considered to have high sensitivity for amplitude reduction of the FRF the same as the MSA for the eigenvalues.

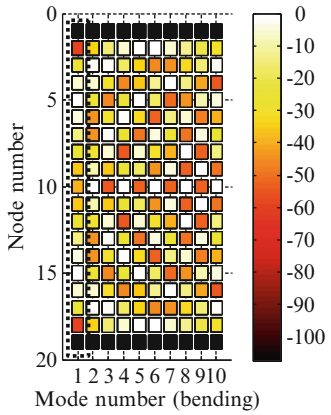

Fig. 13.41 MSA for the eigenvalues

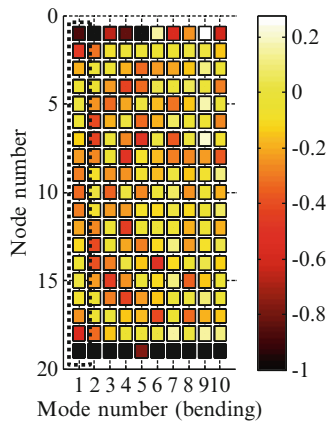

Fig. 13.42 MSA for the amplitude of the FRF

As a result, both ends of the beam are considered to be useful to lower the natural frequency of the first bending mode and to decrease the amplitude of that mode. On the other hand, node #5 or #15 is considered to have small effect on the customization for the first bending mode because these locations have these sensitivities with a value of almost zero which is expected to results as these are close to the node of the mode.

In order to estimate the effect of the modification for the biggest peak, the mass value of the DOFs which were identified to be effective/ineffective for the customization will be modified in the FE model developed. Although the SDM procedure can be applied to the EMA model, because the data from the EMA and FEA have high correlation in the frequency range of interest, only the FEA data will be used here. A 0.5 lb mass is added to for the mass location of experimental node #15 or #19 as a lumped mass, because these locations are considered to be the most effective/ineffective location for the customization of the first mode based on the result of the MSA. The SDM procedure will be used to simulate these two patterns of mass change and the FRFs obtained are shown in Fig. 13.43. In this work, the damping value for the modified system is set to the same as the values measured from the EMA of the original system. In Fig. 13.43, a set of FRFs simulating the mass modification for every experimental node is shown together. From this result, the FRF with the optimal mass change is confirmed to have the greatest effect on the frequency shift and amplitude reduction for the first mode. However, for every mode on the optimal FRF, the amplitude is decreased and the frequency is shifted lower the same as the first mode. This is because the edge of the beam has high sensitivities for every bending mode. On the other hand, the mass modification for the node location, which is #15, changes neither the frequency nor the amplitude of the first mode but, for the other modes, the effect on the frequency shift or amplitude reduction is seen because the sensitivities for the other modes are not small. The detailed modal parameters will be compared between the original and modified model with the experimental results in the next section. Figure 13.44 shows the comparison of the acceleration signals obtained from the original and modified modal parameters using the Newmark method. For both solutions, the same input force shown in Fig. 13.36 is used and the modified signal with the optimal mass modification has lower amplitude than the original signal because the amplitude of the FRF is decreased. Using these modified acceleration signals, the modified SRS can be developed and the result is shown in Fig. 13.45. In this figure, the mass modification for all nodes is also performed the same as Fig. 13.43 so the modified SRSs can be compared to the original SRS and a set of SRSs computed with the acceleration signals with randomized modifications. From this result, the modified SRS computed with the optimal mass modification based on the MSA has the smallest amplitude and

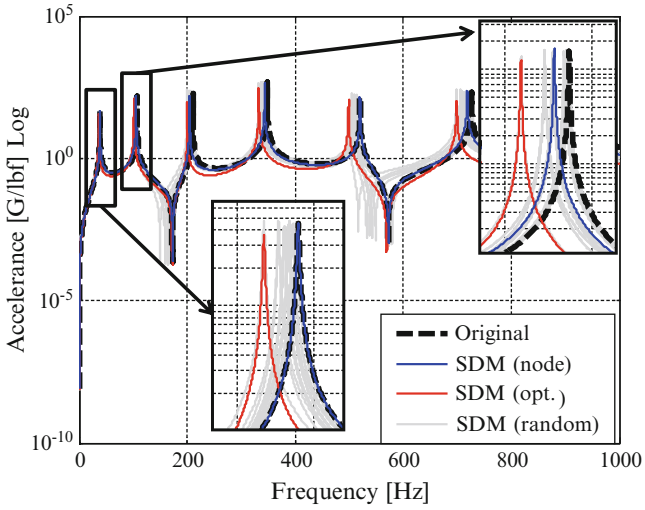

Fig. 13.43 FRF comparison

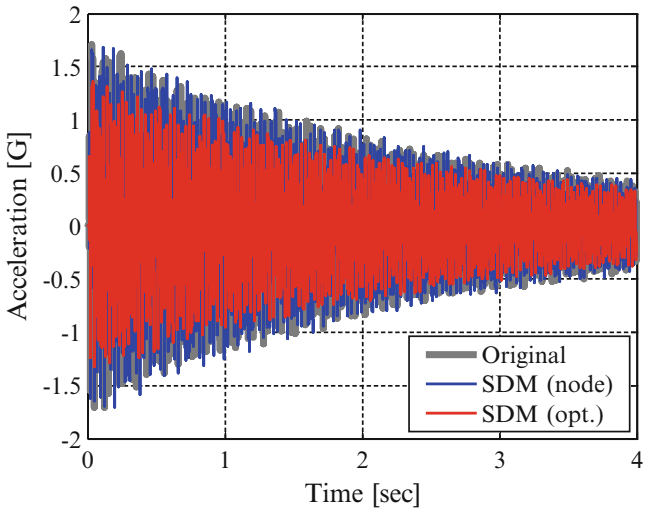

Fig. 13.44 Acceleration signals

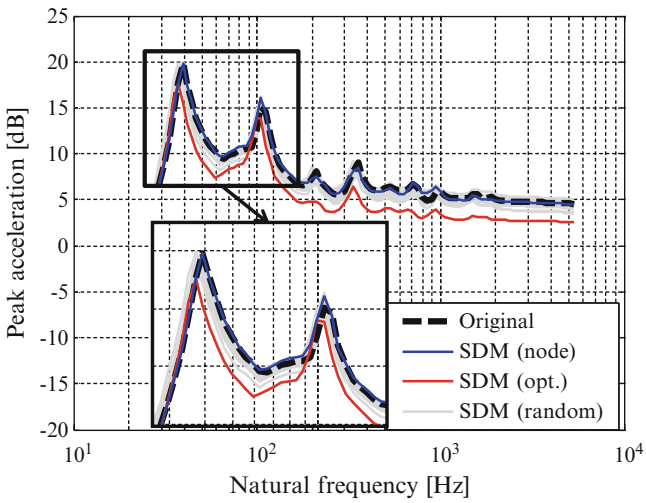

Fig. 13.45 SRS comparison

its frequency shift is the biggest. The amplitude reduction is about 3 dB and the peak frequency is shifted by 4 Hz. But for the SRS with mass modification for the location with small sensitivities, the modified SRS has almost the same peak value as the original SRS at the biggest peak. Due to the result described here, the SRS customization procedure proposed in this work is considered to be valid and useful because the mass modification with high sensitivity values is proved to be useful for the SRS customization and the mass modification with small sensitivity is shown to be not effective.

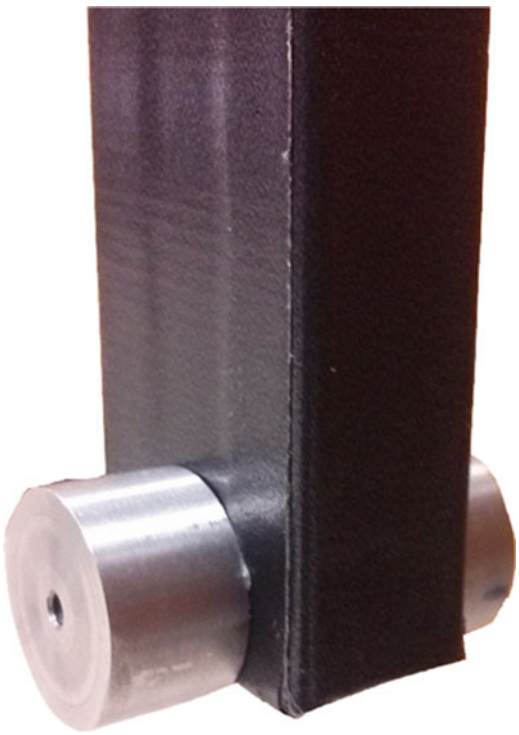

Fig. 13.46 Setup for mass modification

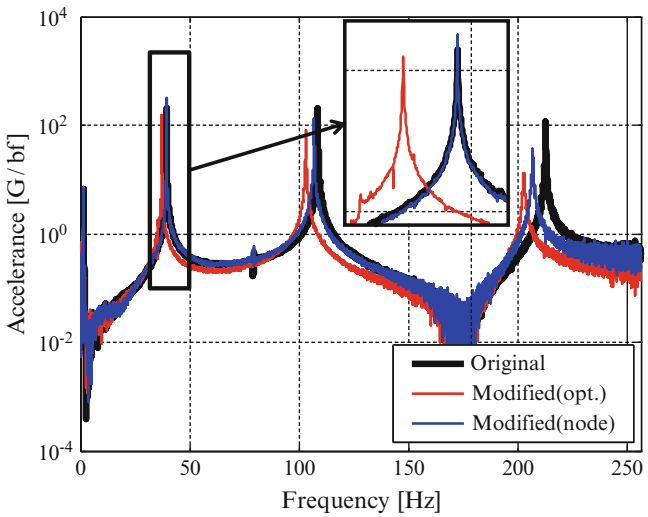

Fig. 13.47 [t] Experimental FRF comparison

In order to check the accuracy of the analytical estimation for the SRS customization, an additional mass will be added to the actual beam system to simulate a SRS customization experimentally. Figure 13.46 shows the experimental setup for conducting the SDM. Two masses each of which has 0.25 lb and that are made of stainless steel is attached to the node #19 and #15 which are considered to have the highest and smallest sensitivities for the first mode. For both of modified systems, a pair of the FRFs will be measured using configuration (i) and the result is shown in Fig. 13.47 compared to the original FRF. From this result, the modified FRF with the optimal mass modification of #19 has lower frequency and smaller amplitude but the modified FRF with the poor location has the same peak specification as the original FRF. Although the added mass is different from the perfect lumped mass condition, this is considered to be reasonable to check the methodology because the FRF modified has the same tendency as the one from the FEA shown in Fig. 13.43, which uses the lumped mass configuration.

In addition, the EMA for the modified system will be performed to obtain the modified modal parameters using the same three configurations used for the measurement for the original model; this is done to obtain the modified modal parameters and compare them with the original one. In this case, only the optimally modified modal parameter is extracted. Table 13.5 shows the result of the EMA and a set of the modified natural frequencies and damping values are shown in the table.

Table 13.5 Modified modal parameters with optimal mass modification

		Natural frequency				Critical damping	
		Modified value (Hz)		Modification effect (%)		Modified value (%)	Modification effect (%)
Mode #	Mode name	EMA	FEA	EMA	FEA	EMA	EMA
3	1st bending	37.265	36.750	−5.83	−6.07	0.3240	16.06
4	2nd bending	102.996	101.856	−5.32	−5.48	0.0713	64.74
5	3rd bending	202.524	200.592	−4.89	−5.01	0.1801	85.29
6	4th bending	334.837	332.899	−4.49	−4.59	0.5246	95.04
7	5th bending	502.690	498.994	−3.72	−4.24	0.6561	96.82
8	6th bending	701.696	699.014	−3.36	−3.93	0.4648	95.85
9	7th bending	929.209	933.065	−3.47	−3.66	0.7685	96.99
10	8th bending	1, 203.610	1, 201.223	−2.20	−3.42	1.0351	96.91
11	9th bending	1, 495.180	1, 503.546	−2.05	−3.18	0.8065	95.71
12	10th bending	1, 819.810	1, 840.082	−1.94	−3.02	0.6595	92.07

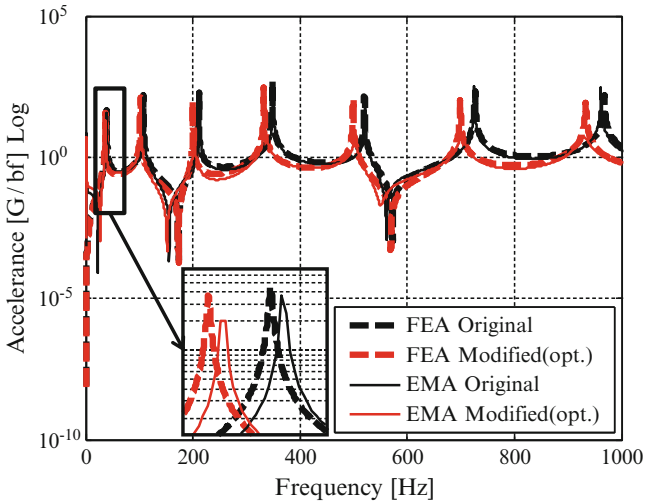

Fig. 13.48 Synthesized FRF for modified system and comparison with FRF from the FEA

Furthermore, the modified natural frequency from the FEA is also shown and the modification effect is calculated based on the change from the original values shown in Tables 13.3 and 13.4. From this result, the change of the experimental natural frequency is similar to the one of the FEA. However, the modified analytical model was assumed to have the same damping as the original system in the process of the analytical modification but the measured damping values after this modification are different from the original values because the mass is added discretely to the structure. Because the actual damping values are hard to estimate before the actual system is built, the original damping values may be able to be used for the estimation of the modified response computation or the modified SRS computation. Using these modal parameters extracted from the EMA, the FRF for the modified system is synthesized using Eq. 13.14 and the result is shown in Fig. 13.48. Because both of the modified FRF from the analytical and experimental solution compare well and both of the modified FRFs have valid modification effect, the modification and the extraction of modal parameter for before/ after the modification are considered to be correct.

In order to develop the SRS for the modified system experimentally, the pendulum shown in Fig. 13.25 will be used to measure the modified acceleration signal and Fig. 13.49 shows the comparison of the input signals used for the original and modified acceleration signal measurement. The measurement will be done for the modified system with the optimal mass modification and the system with the location with small sensitivities. Because these three signals are similar, the modification effect can be judged sufficiently from the measured response signals. Figure 13.50 shows the comparison of the measured response signals before/ after the modification. This result is similar to the analytical result shown in Fig. 13.44.

Finally, the modified SRS will be computed with the measured acceleration signal for the modified model. Figure 13.51 shows the result and the original experimental SRS, the original and modified SRS from the FEA are also shown. The modified SRS with the ineffective location has the same peak value as the original SRS for the biggest peak but, for the modified SRS with the optimal mass location, the peak value is decreased by 2 dB and its frequency is shifted by 2 Hz. The change from the original SRS to the optimally modified SRS in the experiment is similar to the change in the FEA.

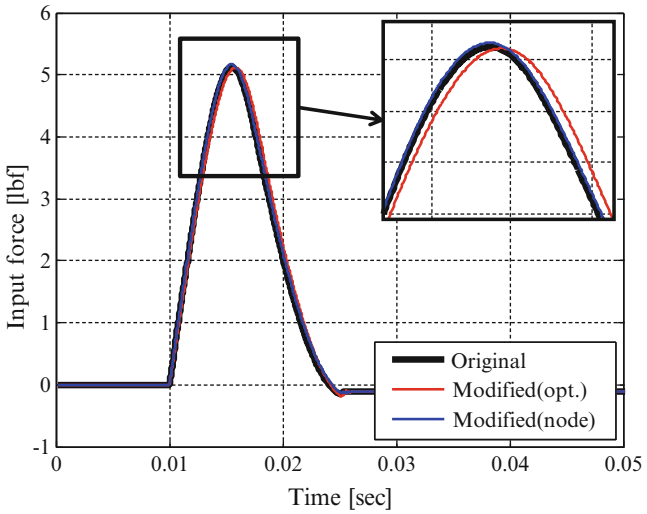

Fig. 13.49 Input force comparison

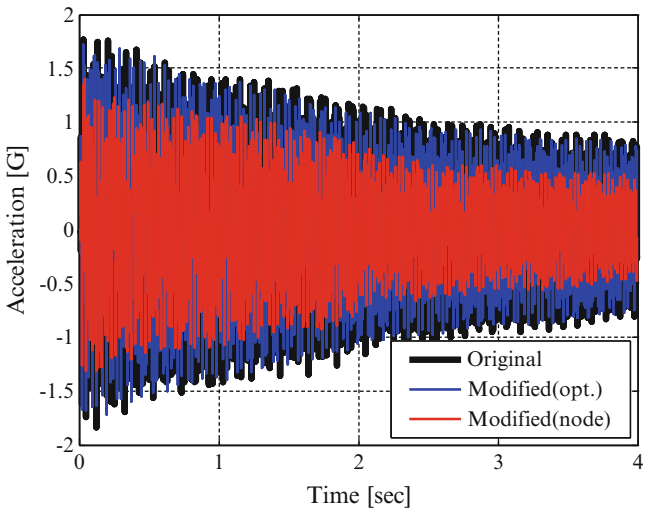

Fig. 13.50 Response signal comparison

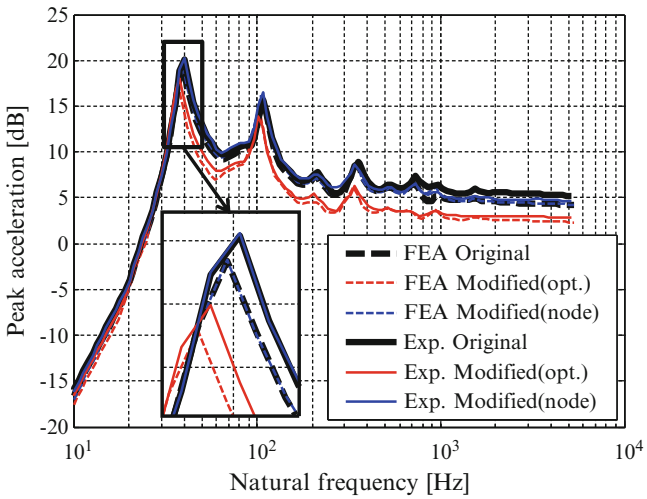

Fig. 13.51 Analytical and experimental SRS for original and modified system

Due to this, the methodology proposed is confirmed with the analytical and experimental solution using the beam model. From both solutions, the modal parameters are compared and the measured modal damping is used for the FE model development for better model description. This method provides the analytical SRS which is very similar to the measured SRS and the modification effect is simulated properly using the FE model developed.

13.6 Conclusion

This paper presents the design methodology for the development of a shock response spectrum test structure that is developed from both analytical and experimental approaches using modal space as a basis for the description of the structure along with the traditional shock response base excitation approach. In addition, the design is further analyzed using both time domain and frequency domain response approaches that are further optimized using structural dynamic modification and mass sensitivity approaches to obtain the desired SRS envelop.

Cases are first presented for a simple 5-DOF analytical model to illustrate all of the techniques described. This is followed by the evaluation of a beam structure using both finite element and experimental modal approaches. Many different cases were evaluated to show all aspects of every approach that is presented in the paper to highlight the effectiveness of each approach. The approaches presented all support the design of a shock response spectrum structure.

Acknowledgements This research was done in the Structural Dynamics and Acoustic Systems Laboratory (SDASL) of the University of Massachusetts Lowell. The first author of this paper is a graduate student of the Acoustic Systems Laboratory (CAMAL) of the Chuo University and visited at the SDASL as a research scholar for a year of 2013 and, at that time, this research was performed. The author would like to thank to Dr. Peter Avitabile for the invitation and invaluable advice and to Dr. Nobuyuki Okubo and Dr. Takeshi Toi for the recommendation for the position.

References

1. NASA-STD-7003A (2011) NASA technical standard-pyroshock test criteria, National Aeronautics and Space Administration, Dec 2011
2. ISO 18431-4 Mechanical vibration and shock-signal processing—part 4: shock response spectrum analysis
3. Tuma J, Koci P (2009) Calculation of shock response spectrum. Colloquium dynamics of machines 2009, Feb 2009
4. Edward Alexander J (2009) Shock response spectrum—a primer. Sound Vib
5. Richard Hsieh et al (2013) Analysis and dynamic characterization of a resonant plate for shock testing. Proceedings of the 31st international modal analysis conference
6. Irvine T An introduction to the shock response spectrum
7. Rao S (2010) Mechanical vibrations, 5th edn. Prentice Hall, New Jersey, pp 968–971
8. Okubo N, Toi T (2000) Sensitivity analysis and its application for dynamic improvement. Sadhana 25(3):291–303
9. Kohei Furuya et al (2005) FRF-sensitivity analysis using eigenvalue analysis of stiffness matrix for a car body structure. Proc. Jpn Soc Automot Eng. No 37-05-188
10. Avitabile P (2001) Twenty years of structural dynamics modification—a review. Proceedings of the 20th international modal analysis conference, Feb 2001
11. ISO 1683-2008 Acoustics—preferred reference values for acoustical and vibratory levels